SYNTHESIS OF NEW FERROCENYL SUBSTITUTED QUINOXALINE DERIVATIVE MONOMERS, THEIR POLYMERIZATION AND ELECTROCHEMICAL BEHAVIORS

A THESIS SUBMITTED TO
THE GRADUATE SCHOOL OF NATURAL AND APPLIED SCIENCES
OF
MIDDLE EAST TECHNICAL UNIVERSITY

BY

ŞERİFE ÖZDEMİR

IN PARTIAL FULFILLMENT OF THE REQUIREMENTS
FOR
THE DEGREE OF MASTER OF SCIENCE
IN
CHEMISTRY

SEPTEMBER 2010

Approval of the thesis:

SYNTHESIS OF NEW FERROCENYL SUBSTITUTED QUINOXALINE DERIVATIVE MONOMERS, THEIR POLYMERIZATION AND ELECTROCHEMICAL BEHAVIORS

submitted by **ŞERİFE ÖZDEMİR** in partial fulfillment of the requirements for the degree of **Master of Science in Chemistry Department, Middle East Technical University** by,

Prof. Dr. Canan Özgen
Dean, Graduate School of **Natural and Applied Sciences**

Prof. Dr. İlker Özkan
Head of Department, **Chemistry**

Prof. Dr. Özdemir Doğan
Supervisor, **Chemistry Dept., METU**

Prof. Dr. Levent Toppare
Co-Supervisor, **Chemistry Dept., METU**

Examining Committee Members:

Prof. Dr. Duygu Kısakürek
Chemistry Dept., METU

Prof. Dr. Özdemir Doğan
Chemistry Dept., METU

Prof. Dr. Levent Toppare
Chemistry Dept., METU

Assoc. Prof. Dr. Adnan Bulut
Chemistry Dept., Kırıkkale University

Assist. Prof. Dr. Ali Çırpan
Chemistry Dept., METU

Date: 17.09.2010

I hereby declare that all information in this document has been obtained and presented in accordance with academic rules and ethical conduct. I also declare that, as required by these rules and conduct, I have fully cited and referenced all material and results that are not original to this work.

Name, Last name : ŞERİFE ÖZDEMİR

Signature

ABSTRACT

SYNTHESIS OF NEW FERROCENYL SUBSTITUTED QUINOXALINE DERIVATIVE MONOMERS, THEIR POLYMERIZATION AND ELECTROCHEMICAL BEHAVIORS

Özdemir, Şerife
M. S., Department of Chemistry
Supervisor: Prof. Dr. Özdemir Doğan
Co-Supervisor: Prof. Dr. Levent Toppare

September 2010, 71 pages

5,8-Bis(2,3-dihydrothieno[3,4b][1,4]dioxin-5-yl)-2-(naphthalen-2-yl)-3-ferrocenyl-4a,8a-dihydroquinoxaline (DEFNQ), 5,8-bis(2,3-dihydrothieno[3,4-b][1,4]dioxin-5-yl)-2-(phenyl)-3 ferrocenylquinoxaline (DEFPQ) and 5,8-bis(2,3-dihydrothieno[3,4-b][1,4]dioxin-5-yl)-2,3-di(naphthalen-2-yl)quinoxaline (DEDNQ) were synthesized, electrochemically polymerized and electrochromic properties of resultant polymers were investigated. For the characterization of the monomers Nuclear Magnetic Resonance (^{1}H-NMR, ^{13}C-NMR) were used. Cyclic Voltammetry (CV) and Ultraviolet–Visible Spectroscopy were used to investigate electrochemical behavior of the monomers and redox reactions of conducting polymers. After electrochemical polymerizations, the electrochromic properties of the conducting polymers were investigated via spectroelectrochemistry, kinetic and colorimetry studies to explore the one of most important property of conducting polymers, the ability to switch reversibly between the two states of different optical properties, 'electrochromism'. Cyclic Voltammetry and Spectroelectrochemistry studies for PDEFNQ, PDEFPQ and

PDEDNQ showed that ferrocenyl (Fc) group containing derivatives are multichromic green to transmissive polymer with high tendency to be both p and n doped. PDEDNQ which was not functionalized with ferrocenyl group does not show multichromism. According to the electrochemical and spectroscopic results each polymer is a potential candidate for optoelectronic applications.

Keywords: Ferrocene, Multichromism, Donor-Acceptor-Donor, Green Polymers, Subsitution Effect.

ÖZ

FEROSENİL SÜBSTİTÜE KİNOKZALİN TÜREVİ MONOMERLERİN SENTEZİ, POLİMERİZASYONU VE ELEKTROKİMYASAL ÖZELLİKLERİNİN İNCELENMESİ

Özdemir, Şerife
Yüksek Lisans, Kimya Bölümü
Tez Yöneticisi: Prof. Dr. Özdemir Doğan
Ortak Tez Yöneticisi : Prof. Dr. Levent Toppare

Eylül 2010, 71 sayfa

5,8-Bis(2,3-dihydrothieno[3,4b][1,4]dioxin-5-yl)-2-(naphthalen-2-yl)-3-ferrocenyl-4a,8a-dihydroquinoxaline (DEFNQ), 5,8-bis(2,3-dihydrothieno[3,4-b][1,4]dioxin-5-yl)-2-(phenyl)-3 ferrocenylquinoxaline (DEFPQ) ve 5,8-bis(2,3-dihydrothieno[3,4-b][1,4]dioxin-5-yl)-2,3-di(naphthalen-2-yl)quinoxaline (DEDNQ) monomerleri sentezlenmiş, elektrokimyasal olarak polimerleştirilmiş ve elde edilen polimerlerin elektrokimyasal özellikleri incelenmiştir. Sentezlenen monomerlerin karakterizasyonu için ^{1}H, ^{13}C Nükleer Manyetik Rezonans Spektroskopisi (NMR) kullanılmıştır. Dönüşümlü Voltammetre (CV) ve UV-Vis Spektrofotometresi kullanılarak monomerlerin elektrokimyasal davranışı ve iletken polimerlerin redox tepkimeleri tespit edilmiştir. Elektrokimyasal polimerizasyon sonucunda elde edilen iletken polimerlerin elektrokromik özellikleri spektroelektrokimya, kinetik ve kolorimetri çalışmaları sonucunda incelenmiş ve bu kısımda iletken polimerlerin en ilginç özelliklerinden biri olan ‘electrokromizm’ araştırılmıştır. Dönüşümlü Voltametre ve

Spektroelektrokimya çalışmaları sonucunda Ferrosenil (Fc) grup içeren türevlerin (PDEFNQ, PDEFPQ) indirgenmiş halde yeşil yükseltgenince yüksek geçirgenliğe sahip olduğu ve aynı zamanda multikromik özellik gösterdiği gözlenmiştir. Ferrosenil grubu içermeyen türevin (PDEDNQ) ise multikromik özellik göztermediği gözlenmiştir. Tüm polimerler hem p-tipi hem n-tipi katkılanabilmektedir. Elektrokimysal ve spektroskopik sonuçlar her bir polimerin optoelektronik uygulamalar için iyi birer aday olduğunu göztermektedir.

Anahtar kelimeler: Ferrosen, Multikromizm, Donör-Akseptör-Donör, Yeşil Polimerler, Substitüsyon Etkisi.

To My Family

ACKNOWLEDGEMENTS

I would like to express my sincere thanks to my supervisor Prof. Dr. Özdemir Doğan and my co-supervisor Prof. Dr. Levent Toppare for their guidance, support, encouragement, patience, advice, criticism and for listening and helping me in many ways.

I would like to thank to Abidin Balan and Derya Baran for their endless helps besides their kind friendships.

I would like to thank to Assoc. Prof. Dr. Adnan Bulut for his valuable discussions and friendship.

I would like thank to Hakan Babiz, Akın İnce, Gül Şenyurt, Muhammet İşçi and all Toppare Research Group members for their cooperation and their kind friendships.

Many thanks to Yadigar, Hacer, Dilek, Naime for always being there for me, for their true friendship.

Words fail to express my eternal gratitude to my family for believing in me and giving me endless support.

I would like to express my special thanks to Fırat Hacıoğlu. I always know that he is with me and he never leaves me alone.

TABLE OF CONTENTS

ABSTRACT iv

ÖZ vi

ACKNOWLEDGEMENTS ix

TABLE OF CONTENTS x

LIST OF TABLES xiii

LIST OF FIGURES xiv

ABBREVATIONS xix

CHAPTERS

1.INTRODUCTION 1

- 1.1 Conducting Polymers 1
- 1.2 Band Theory 2
- 1.3 Doping Types in Conducting Polymers 6
- 1.4 Polymerization methods 8
- 1.5 Applications of Conducting Polymers 10
- 1.6 Electrochromism 11
  - 1.6.1 Types of Electrochromic Materials 12
  - 1.6.2 Multicolor Electrochromic Polymers: Color Control 14
- 1.7 Low Band Gap Systems 15
- 1.8 Color of Conducting Polymers and Impotance of Green Polymeric Materials 17
- 1.9 Ferrocene Polymers 19
- 2.EXPERIMENTAL 24
- 2.1 Materials and Methods 24
- 2.2 Equipment 24
- 2.3 Procedure, Synthesis 25

2.3.1 Synthesis of 2-Hydroxy-2-(naphthalen-2-yl)-1-ferrocenylethanone 25
2.3.2 Synthesis of 1-ferrocenyl-2-naphthylethanedione 26
2.3.3 Synthesis of 1-ferrocenyl-2-phenylethanedione 26
2.3.4 Synthesis of 1,2-di(naphthalen-2-yl)ethane-1,2-dione............................. 27
2.3.5 Synthesis of 4,7-Dibromo-2.1.3-benzothiadiazole................................... 28
2.3.6 Synthesis of 3,6-dibromo-1,2-phenylenediamine 28
2.3.7 Synthesis of tributl(2,3-dihydrothieno[3,4-b][1,4]dioxin-5-yl)stannane .. 29
2.3.8 Synthesis of 5,8-dibromo-2-(naphthalen-2-yl)-3-ferrocenyl-4a,8a-dihydroquinoxaline 30
2.3.9 Synthesis of 5,8-bis(2,3-dihydrothieno[3,4-b][1,4]dioxin-5-yl)-2-(naphthalen-2-yl)-3-ferrocenyl-4a,8a-dihydroquinoxaline (M1)....................... 31
2.3.10 Synthesis of 5,8-dibromo-2-phenyl-3-ferrocenylquinoxaline................. 32
2.3.11 Synthesis of 5,8-bis(2,3-dihydrothieno[3,4-b][1,4]dioxin-5-yl)-2-(phenyll)-3-ferrocenylquinoxaline (M2)... 32
2.3.12 Synthesis of 5,8-dibromo-2,3-di(naphthalen-2-yl)quinoxaline............... 34
2.3.13 Synthesis of 5,8-bis(2,3-dihydrothieno[3,4-b][1,4]dioxin-5-yl)-2,3-di(naphthalen-2-yl)quinoxaline (M3).. 35

3.RESULTS AND DISCUSSION 36

3.1 Electrochemical and Electrochromic Properties of Quinoxaline Derivative ... 36
Polymers.. 36
3.1.1 Electrochemical and Electrochromic Properties of PDEFNQ (P1) 36
3.1.1.1 Electrochemistry of DEFNQ (M1).. 36
3.1.1.2 Spectroelectrochemistry of P1 40
3.1.1.3 Kinetic Studies of P1... 42
3.1.2 Electrochemical and Electrochromic Properties of PDEFPQ (P2)........... 43
3.1.2.1 Electrochemistry of DEFPQ (M2) 43
3.1.2.2 Spectroelectrochemistry of P2 45
3.1.2.3 Kinetic Studies of P2... 47
3.1.3 Electrochemical and Electrochromic Properties of PDEDNQ (P3).......... 48
3.1.3.1 Electrochemistry of DEDNQ (M3).. 48
3.1.3.2 Spectroelectrochemistry of P3 50

3.1.3.3 Kinetic Studies of P3 51

3.2 Comparison of PDEFNQ (P1), PDEFPQ (P2), PDEDNQ (P3) and PDPEQ .. 53

4.CONCLUSION 55

REFERENCES 56

APPENDIX A - NMR DATA 61

LIST OF TABLES

TABLES

Table 1 Electrochemical and Optical Results for P1, P2, P3 and PDPEQ . [a] Data was Taken from Ref 69. [b] Fc/Fc$^+$ Oxidation Potential was Observed in The First Cycle During CV. 54

LIST OF FIGURES

FIGURES

Figure 1. 1 Common Conjugated Polymers 2
Figure 1. 2 The Band Structure of an Insulator, a Semiconductor and a Conductor .. 3
Figure 1. 3 The Degenerate Ground States of Pa (a) and the Nondegenerate Ground States of The Fully Aromatic Polymer, Poly(P-Phenylene) (b). 4
Figure 1. 4 The Charged States, Charge Carries and Energy Bands for Pa [8]. 5
Figure 1. 5 The Charged States, Charge Carries and Energy Bands for Poly(Thiophene) [8]. 6
Figure 1. 6 Band Model of (A) Non-Doped, (B) Slightly Doped, and (C) Heavily Doped Conducting Polymers. 7
Figure 1. 7 a) p-Doping and b) n-Doping of Conducting Polymer 8
Figure 1. 8 Radical-Cation/Monomer and Radical-Cation/Radical Cation Coupling 9
Figure 1. 9 Electrochemical Polymerization Mechanism for a Five Membered Heterocyclic Compound, Where X = N-H, S, O 10
Figure 1. 10 The Three Common Viologen Redox States, Dication, Radical Cation, Neutral Species. 12
Figure 1. 11 The Doped and Undoped Form of Polypyrrole. 13
Figure 1. 12 Examples of Multicolor Ec Polymers Synthesized by Structural Modification. 0 = Neutral; I= Intermediate; + =Oxidized; - and-- = Reduced 15
Figure 1. 13 Illustration of methods for the alteration of band gap 16
Figure 1. 14 VB and CB Levels for Cyanovinylene Subsituted with Different Donor Groups. 17
Figure 1. 15 Structure of The First Neutral State Green Polymer............................ 18
Figure 1. 16 Examples of Gren Polymeric Materials With Transmissive Oxidized State. 19

Figure 1. 17 Structure of Ferrocene. 19
Figure 1. 18 Schematic Representation of Three Types of Metal Containing Conducting Polymers. 21
Figure 1. 19 Synthetic Route to Ferrocene Clicked Poly(3,4-Ethylenedioxythiophene). 22
Figure 1. 20 Structures of a) 1,1-Bis(5-(2,2-Bithienyl))Ferrocene and b) 1,1-Bis(5-(2,2:5,2-Terthienyl)) Ferrocene. 22

Figure 2. 1 Synthetic Route for 2-Hydroxy-2-(Naphthalen-2-yl)-1-Ferrocenylethanone 25
Figure 2. 2 Synthetic Route for 1-Ferrocenyl-2-Naphthylethanedione 26
Figure 2. 3 Synthetic Route for 1-Ferrocenyl-2-Phenylethanedione 26
Figure 2. 4 Synthetic Route for 1,2-Di(Naphthalen-2-yl)Ethane-1,2-Dione 27
Figure 2. 5 Synthetic Route for 4,7-Dibromo-2.1.3-Benzothiadiazole 28
Figure 2. 6 Synthetic Route for 3,6-Dibromo-1,2-Phenylenediamine 28
Figure 2. 7 Synthetic Route for Tributyl(2,3-Dihydrothieno[3,4-b][1,4]Dioxin-5-yl)Stannane 29
Figure 2. 8 Synthetic Route for 5,8-Dibromo-2-(Naphthalen-2-yl)-3-Ferrocenyl-4a,8a-Dihydroquinoxaline: 30
Figure 2. 9 Synthetic Route for 5,8-Bis(2,3-Dihydrothieno[3,4-B][1,4]Dioxin-5-yl)-2-(Naphthalen-2-yl)-3-Ferrocenyl-4a,8a-Dihydroquinoxaline 31
Figure 2. 10 Synthetic Route for 5,8-Dibromo-2-Phenyl-3-Ferrocenylquinoxaline 32
Figure 2. 11 Synthetic Route for 5,8-Bis(2,3-Dihydrothieno[3,4-B][1,4]Dioxin-5-yl)-2-(Phenyll)-3-Ferrocenylquinoxaline 33
Figure 2. 12 Synthetic Route for 5,8-Dibromo-2,3-Di(Naphthalen-2-yl)Quinoxaline 34
Figure 2. 13 Synthetic Route for 5,8-Bis(2,3-Dihydrothieno[3,4-B][1,4]Dioxin-5-yl)-2,3-Di(Naphthalen-2-yl)Quinoxaline 35

Figure 3. 1 Single Scan Voltammograms of A) Fc — , Acceptor Unit — In Acn and B) The First Run Of Electropolymerization of M1 in a Dcm/Acn (5:95,V:V)/ TBAPF6 Solvent-Electrolyte Couple. 37

Figure 3. 2 Multiple Scan Voltammogram for Polymerization of M1 in Dcm/Acn/ TBAPF6 Solution. 38
Figure 3. 3 Single Scan Voltammogram of P1 Upon Both p and n-Type Doping.... 39
Figure 3. 4 Scan Rate Dependence of P1 Films At 100, 150, 200, 250, and 300 mV/s. 39
Figure 3. 5 Electronic Absorption Spectra for PDEFNQ Upon p Doping Between -0.3 V and 1.2 V with 0.1 V Potential Intervals in a Monomer Free Solution. 41
Figure 3. 6 Colors of P1 at its Neutral (0.0 V) and Different Oxidized States. 41
Figure 3. 7 Percent Transmittance Changes as a Function of Time At 730 nm and 1750 nm for P1. 42
Figure 3. 8 Repeated Potential Scan Electropolymerization of M2 in 0.1 M TBAPF6/ACN/DCM on ITO Electrode. 43
Figure 3. 9 Single Scan Voltammogram of P2 Upon Both p and n-Type Doping.... 44
Figure 3. 10 Scan Rate Dependence of P2 Films at 100, 150, 200, 250, and 300 mV/s. 45
Figure 3. 11 Electronic Absorption Spectra for PDEFPQ upon p Doping Between -0.5 V and 1.0 V with 0.1 V Potential Intervals in a Monomer Free Solution. 46
Figure 3. 12 Colors of P2 At Its Neutral (0.0 V) and Different Oxidized States 46
Figure 3. 13 Percent Transmittance Changes as a Function Of Time At 703 nm and 1700 nm for P2. 47
Figure 3. 14 Repeated Potential Scan Electropolymerization of M2 in 0.1 M TBAPF6/ACN/DCM on ITO Electrode. 48
Figure 3. 15 Single Scan Voltammogram of P3 Upon Both p and n-Type Doping.. 49
Figure 3. 16 Scan Rate Dependence of P3 Films At 100, 150, 200, 250, and 300 mV/s. 49
Figure 3. 17 Electronic Absorption Spectra for PDEDNQ Upon p Doping Between -0.5 V And 1.0 V With 0.1 V Potential Intervals in a Monomer Free Solution. 50
Figure 3. 18 Colors of P3 at its Neutral (0.0 V) and Oxidized State. 51
Figure 3. 19 Percent Transmittance Changes as a Function of Time at 450 Nm, 760 nm and 1800 nm for P3. 52
Figure 3. 20 Chemical Structures of P1, P2, P3 And PDPEQ 53

Figure A. 1 ^{1}H-Nmr Spectrum of 2-Hydroxy-2-(Naphthalen-2-yl)-1-Ferrocenylethanone **3** 61

Figure A. 2 ^{13}C-Nmr Spectrum of 2-Hydroxy-2-(Naphthalen-2-yl)-1-Ferrocenylethanone **3** 62

Figure A. 3 ^{1}H-Nmr Spectrum of 1-Ferrocenyl-2-Naphthylethanedione **4** 62

Figure A. 4 ^{1}H-Nmr Spectrum of 1-Ferrocenyl-2-Phenylethanedione**7** 63

Figure A. 5 ^{13}C-Nmr Spectrum of 1-Ferrocenyl-2-Phenylethanedione **7** 63

Figure A. 6 ^{1}H-Nmr Spectrum of 1,2-Di(Naphthalen-2-yl)Ethane-1,2-Dione **9** 64

Figure A. 7 ^{1}H-Nmr Spectrum of 4, 7-Dibromo-2.1.3-Benzothiadiazole **11** 64

Figure A. 8 ^{13}C-Nmr Spectrum of 4, 7-Dibromo-2.1.3-Benzothiadiazole **11** 65

Figure A. 9 ^{1}H-Nmr Spectrum of 3,6-Dibromo-1,2-Phenylenediamine **12** 65

Figure A. 10 ^{13}C-Nmr Spectrum of 3, 6-Dibromo-1, 2-Phenylenediamine **12** 66

Figure A. 11 ^{1}H-Nmr Spectrum of 5, 8-Dibromo-2-(Naphthalen-2-yl)-3-Ferrocenyl-4a, 8a-Dihydroquinoxaline **15** 66

Figure A. 12 ^{13}C-Nmr Spectrum of 5,8-Dibromo-2-(Naphthalen-2-yl)-3-Ferrocenyl-4a,8a-Dihydroquinoxaline **15** 67

Figure A. 13 ^{1}H-Nmr Spectrum of 5,8-Bis(2,3-Dihydrothieno[3,4-B][1,4]Dioxin-5-yl)-2-(Naphthalen-2-yl)-3-Ferrocenyl-4a,8a-Dihydroquinoxaline **M1** 67

Figure A. 14 ^{13}C-Nmr Spectrum of 5,8-Bis(2,3-Dihydrothieno[3,4-B][1,4]Dioxin-5-yl)-2-(Naphthalen-2-yl)-3-Ferrocenyl-4a,8a-Dihydroquinoxaline **M1** 68

Figure A. 15 ^{1}H-Nmr Spectrum of 5,8-Dibromo-2-Phenyl-3-Ferrocenylquinoxaline **16** 68

Figure A. 16 ^{13}C-Nmr Spectrum of 5,8-Dibromo-2-Phenyl-3-Ferrocenylquinoxaline **16** 69

Figure A. 17 ^{1}H-Nmr Spectrum of 5, 8-Bis (2, 3-Dihydrothieno [3, 4-B][1,4]Dioxin-5-yl)-2-(Phenyll)-3-Ferrocenylquinoxaline **M2** 69

Figure A. 18 ^{13}C-Nmr Spectrum of 5, 8-Bis (2, 3-Dihydrothieno [3, 4-B][1,4]Dioxin-5-yl)-2-(Phenyll)-3-Ferrocenylquinoxaline **M2** 70

Figure A. 19 ^{1}H-Nmr Spectrum of 5,8-Dibromo-2,3-Di(Naphthalen-2-yl)Quinoxaline **17** 70

Figure A. 20 ^{1}H-Nmr Spectrum of 5,8-Bis(2,3-Dihydrothieno[3,4-B][1,4]Dioxin-5-yl)-2,3-Di(Naphthalen-2-yl)Quinoxaline **M3** 71

Figure A. 21 ^{13}C-Nmr Spectrum of 5,8-Bis(2,3-Dihydrothieno[3,4-B][1,4]Dioxin-5-yl)-2,3-Di(Naphthalen-2-yl)Quinoxaline **M3** 71

ABBREVATIONS

ACN	Acetonitrile
CB	Conduction Band
CP	Conducting Polymer
CV	Cyclic Voltammetry
DCM	Dichloromethane
ECD	Electrochromic Device
EDOT	3,4-Ethylenedioxythiophene
E_g	Band Gap Energy
Fc	Ferrocenyl
HOMO	Highest Occupied Molecular Orbital
ITO	Indium Tin Oxide
LED	Light Emitting Diode
LUMO	Lowest Unoccupied Molecular Orbital
NMR	Nuclear Magnetic Resonance
PDEQ	Poly5,8-Bis(2,3-dihydrothieno[3,4-b][1,4]dioxin-5-yl)
PDEFNQ	5,8-bis(2,3-dihydrothieno[3,4-b][1,4]dioxin-5-yl)-2-(naphthalen-2-yl)-3-ferrocenyl-4a,8a-dihydroquinoxaline
PDEFPQ	5,8-bis(2,3-dihydrothieno[3,4-b][1,4]dioxin-5-yl)-2-(phenyll)-3-ferrocenylquinoxaline
PDEDNQ	5,8-bis(2,3-dihydrothieno[3,4-b][1,4]dioxin-5-yl)-2,3-di(naphthalen-2-yl)quinoxaline
PPy	Polypyrrole
PTh	Polythiophene
PTSA	P-toluene sulfonic acid
$TBAPF_6$	Tetrabutylammonium hexafluorophosphate
VB	Valence Band

CHAPTER 1

INTRODUCTION

1.1 Conducting Polymers

Electronically conducting polymers are active materials whose properties can be changed as a result of their electrochemical potential [1]. Investigation of polymers having high electronic conductivity in the partially oxidized state opened a new era in the 1970s and promising optical and electrical properties of conducting polymers increase an interest in organic semiconductor materials [2].

Shirakawa and coworkers prepared polyacetylene and its conductivity after doping was discovered by MacDiarmid and Heeger [3]. Alan Heeger, Alan MacDiarmid, and Hideki Shirakawa received the Nobel Prize in Chemistry in year 2000 "for the discovery and development of electrically conductive polymers”

A new class of materials named as synthetic metals were generated as a result of this superior discovery, that conjugated polymers can be converted into metals upon doping. New classes of conducting polymers such as polythiophenes, polypyrroles and many others were developed and electrochemistry played an important role during the preparation and characterization of these original materials. The polyheterocycles have gathered substantial attention because of their electron-rich character which makes their oxidation eaiser. Another advantage of polyheterocycles is their structural complexity which makes structural modifications possible and improves processability [4].

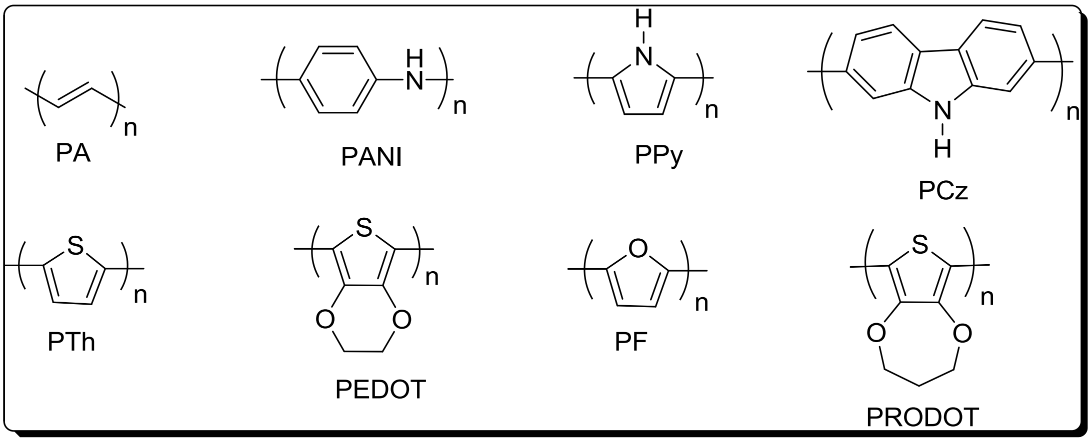

Figure 1. 1 Common conjugated polymers

1.2 Band Theory

Electronically conducting polymers are widely conjugated molecules and their electronic structures can be defined as delocalized band-like structure. Band theory can explain the electronic structure of materials which are defined as insulators, semiconductors, or metals. The major difference between these materials is band gap (E_g) which can be described as the energy spacing between the highest occupied and lowest unoccupied band. Metals have partially filled bands resulting the free movement of charge carriers. This free movement makes metals conducting. On the other hand, insulators have large band gap between two bands. Semiconductors have a filled valence band and an empty conduction band with a narrow band gap (E_g) and so electrons can move to conduction band by thermally or photochemically. As a result, in order to increase conductivity semiconductors can be doped. This doping process can be done with dopants either holes (p-type) or electrons (n-type) which are also called as charge carriers[5].(Figure 1.2)

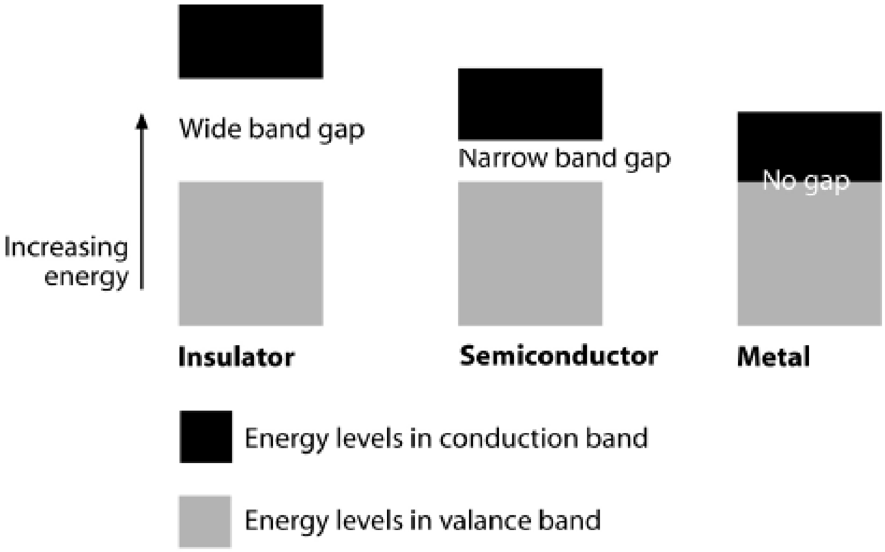

Figure 1. 2 The band structure of an insulator, a semiconductor and a conductor

Polyacetylene (PA) which is the simplest conducting polymer or poly(p-phenylene) and polythiophene which are more complicated with respect to PA can be used to understand band theory of conducting polymers more clearly.

PA is a simple chain of sp^2 *hybridized carbon atoms with alternating single and double bonds leading to two degenerate neutral resonance structures* [6]. As a result of wide delocalization, all the bond lengths are equal in PA, whereas, in aromatic polymers like poly(p-phenylene), two nondegenerate ground states exist [7].

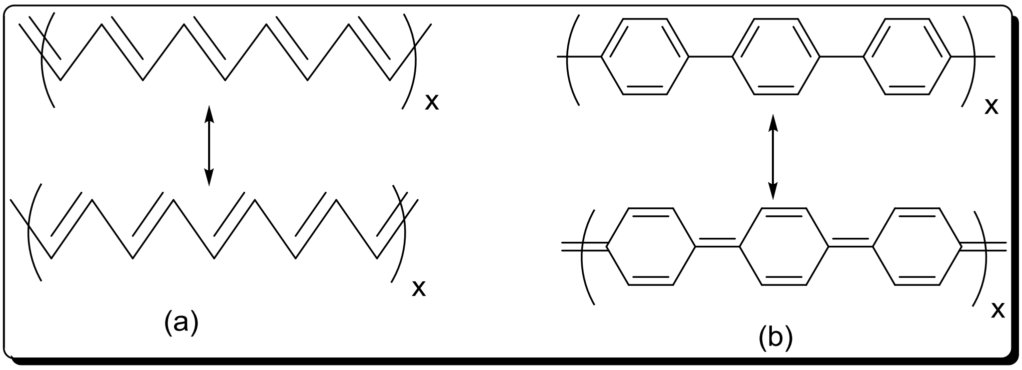

Figure 1. 3 The degenerate ground states of PA (a) and the nondegenerate ground states of the fully aromatic polymer, poly(p-phenylene) (b).

For PA as conjugation increases a band structure formation is observed. The ground state of polyacetylene is degenerate which produces structural defects in polymer chains. These defects cause a change in bond alternation. At the defect site, a single unpaired electron exists and this neutral defect known as a 'soliton'. A minimum energy configuration can be achieved by combaining a neutral soliton and a charged one. These two will produce a 'polaron' , which can be defined as a radical cation, and polaron brings about two states in the band gap, a bonding and an anti-bonding orbital. At a high doping level, two charged solitons will form as a combination of polarons. And finally the interaction of charged solitons will form a soliton band which creates metallic conductivity [5].

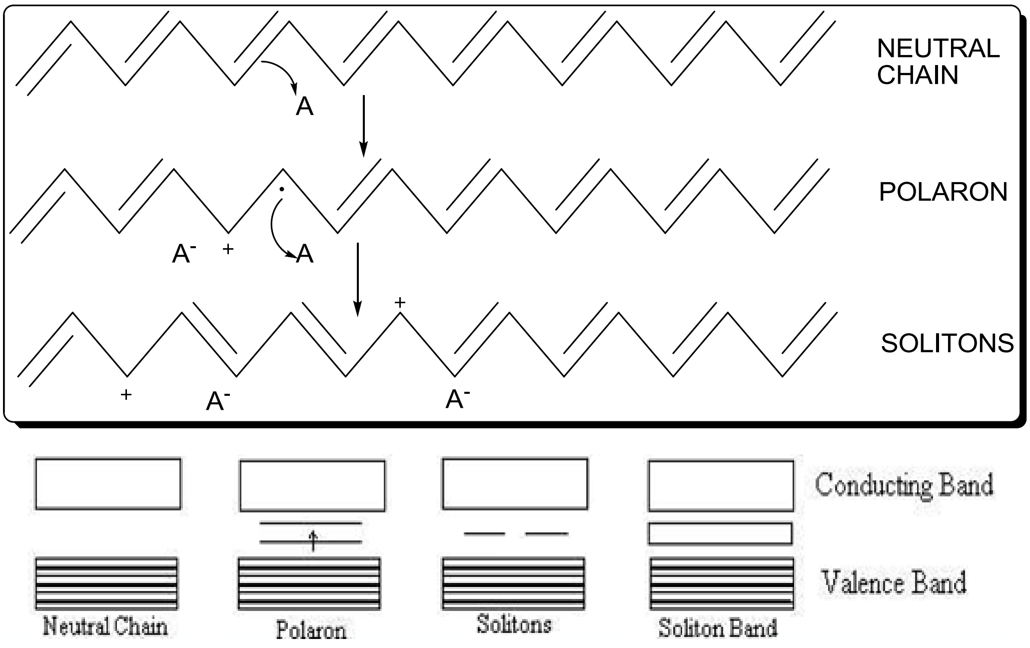

Figure 1. 4 The charged states, charge carries and energy bands for PA [8].

All other conjugated polymers have non-degenerate ground states and so the situation is different during doping process. We can illustrate these differences by comparing oxidation of polpyrrole with PA. In this case polarons, in other words radical cations, are the main charge carriers during the first oxidation. Further oxidation results the combination of two polarons and formation of dications called as bipolarons. At higher doping levels, bipolarons may also combine to form 'bipolaron bands' which are responsible for electrical conductivity in conjugated polymers [9,10].

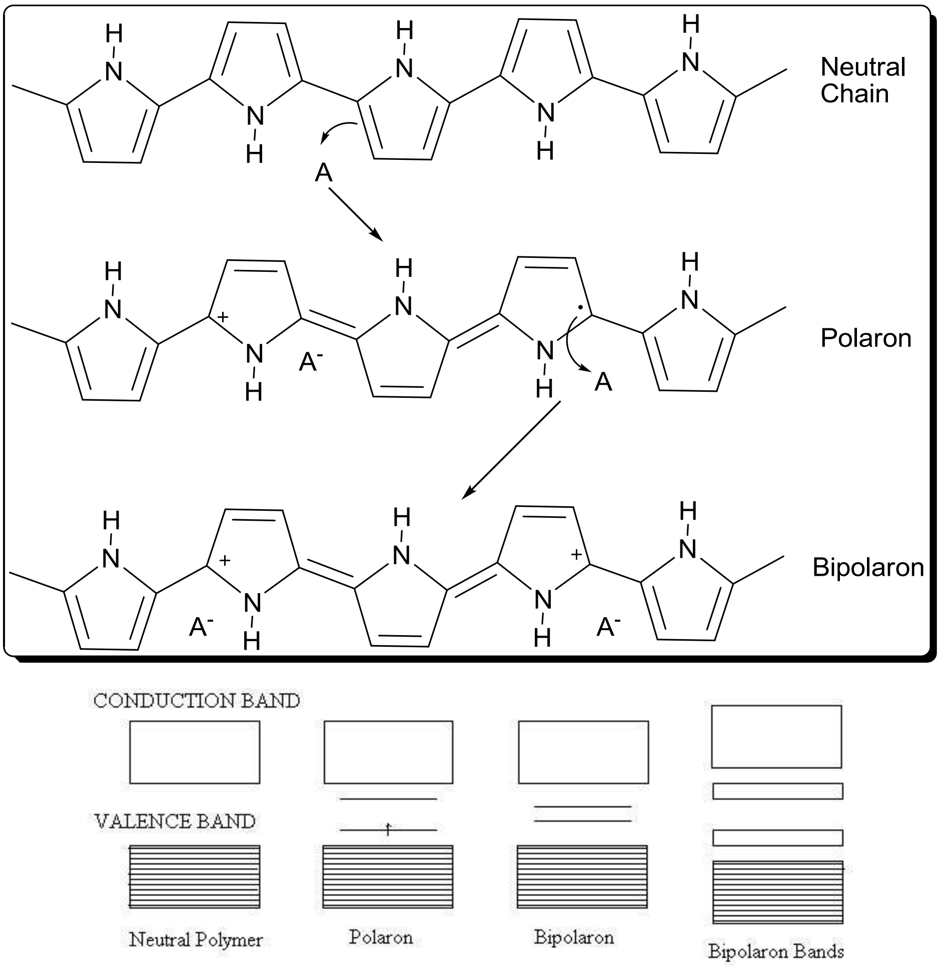

Figure 1. 5 The charged states, charge carries and energy bands for poly(pyrrole) [8].

1.3 Doping Types in Conducting Polymers

Conjugated polymers are insulator in neutral state but conductivity can be achieved by doping process. *Doping can be defined as injection (ejection) of charge to (from) the polymer chain and should be reversible* [11]. Conductivity can be adjusted by changing doping level between neutral polymer and heavily doped polymer [12].

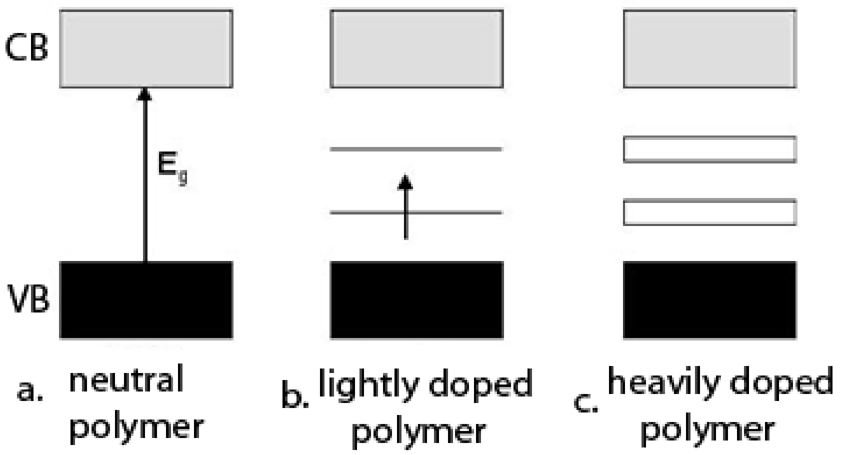

Figure 1. 6 Band model of (a) non-doped, (b) slightly doped, and (c) heavily doped conducting polymers.

Doping process can be performed by chemical, photochemical, interfacial or electrochemical ways. Between them electrochemical doping is most easy and processable way in order to control doping process [11].

Electrochemical doping, which changes electronic strucure of conducting polymers via oxidation or reduction, can be done by applying suitable potentials to the polymer. P-doping and n-doping are the two methods for doping process. The former one, p-doping, can be defined as extraction of an electron from its valence band or oxidation of the neutral polymer. The latter one, n-doping, can be described as insertion of an electron to its conduction band or reduction. Whether p-doping or n-doping will take place can be determined by comparing the position of Fermi level of the substrate ($E_{F,m}$) with the valence band ($E_{VB,p}$) and the conduction band ($E_{CB,p}$) of the polymer [13].

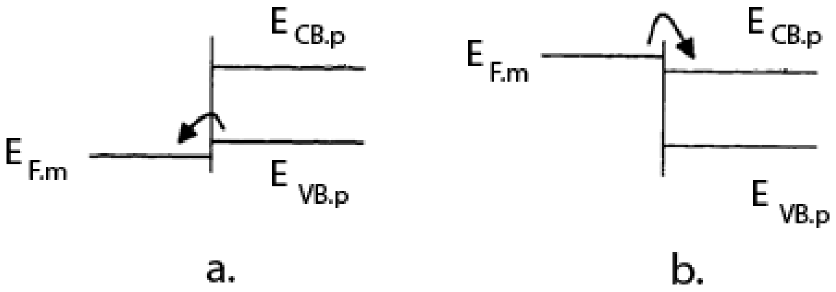

Figure 1. 7 a) p-doping and b) n-doping of conducting polymer

Study on p-doping process is easier then n-doping because the dry and oxygen free medium is required for n-doping studies [14]. Otherwise the oxidation of negatively charged polymers takes place easily. As a result, in the literature number of studies about n-doping is less then p-doping studies [15-17].

1.4 Polymerization methods

Synthesis of conducting polymers can be done by using the different techniques such as; Chemical polymerization, electrochemical polymerization, photochemical polymerization, metathesis polymerization, concentrated emulsion polymerization, inclusion polymerization, solid-state polymerization, plasma polymerization, pyrolysis, soluble precursor polymer preparation [18].

Chemical polymerization is usually prefered for synthesizing large amounts of conducting polymers because electrodes are not required for this type of polymerization [18].

If we compare chemical and electrochemical polymerization, the latter has a lot of advantages over the former. For electrochemical polymerization rapid characterization of conducting polymers are posssible because in this case desired polymers synthesized on an electrode surface. In addition it is simple, reproducible and the film thickness can be controlled during electrochemical polymerization [11].

Figure 1.9 shows the electrochemical polymerization mechanism for a five membered heterocyclic compound. The first step is oxidation of the monomer which is electrochemical (E) process and gives radical cation. For the second process, which is chemical (C), there are two possibilities. The first one is radical cation-radical cation coupling yielding dication. The second possibility is radical cation-monomer coupling followed by oxidation to a dimeric heterocycle dication. Then elimination of two protons take place and aromaticity is regained. After dimers formed near the electrode surface, oxidation of these dimers take place by the help of applied potential which yields again radical cations. Coupling of them gives trimer, etc [19].

As a result, this polymerization mechanism is named as ECE process [Niziurski-Mann 1993] E and C indicates electrochemical and chemical process [19].

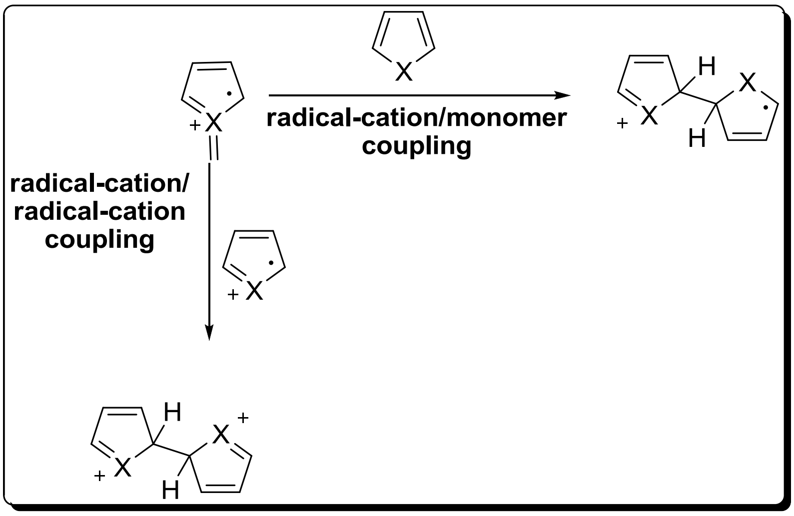

Figure 1. 8 Radical-cation/monomer and radical-cation/radical cation coupling

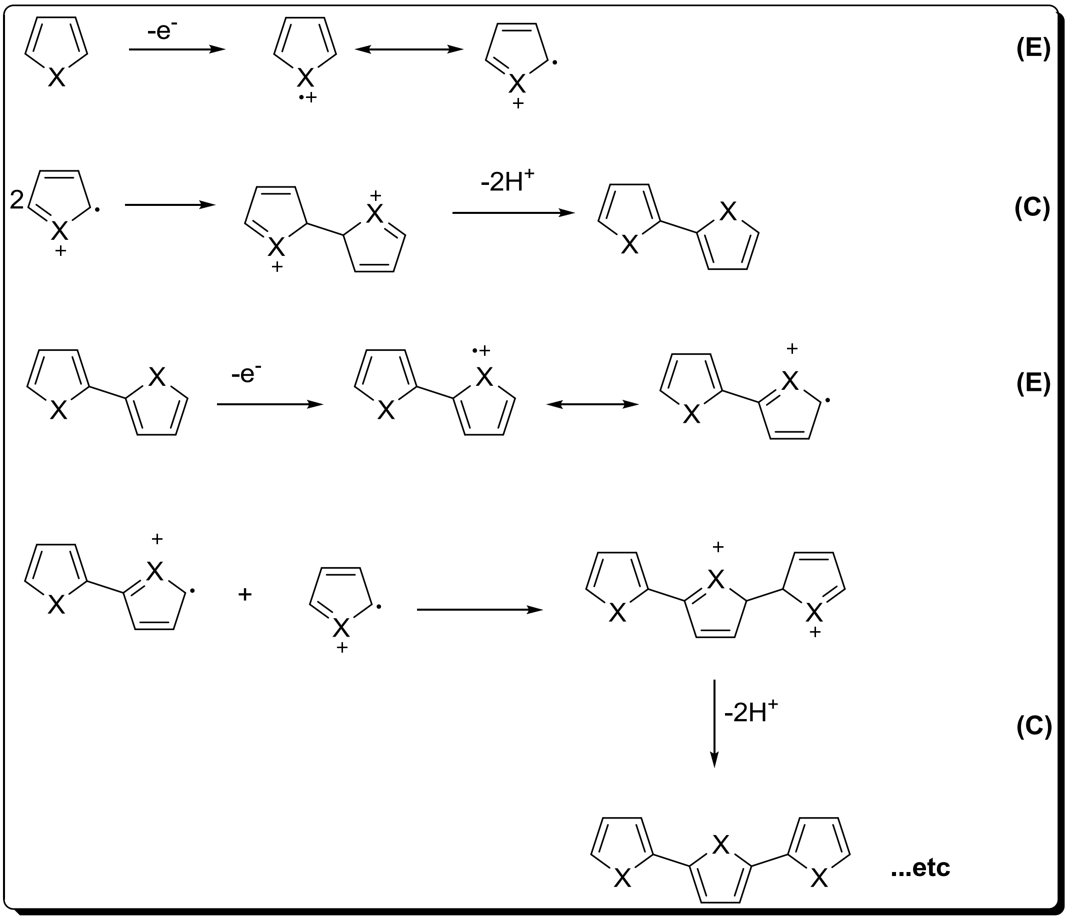

Figure 1. 9 Electrochemical polymerization mechanism for a five membered heterocyclic compound, where X = N-H, S, O

1.5 Applications of Conducting Polymers

Investigation of conducting polymers opened a new research area which is very fascinating due to several advantages such as; low cost, ease of processability, rapid response times, high optical contrasts and color variety [20].

Conducting polymers can be prepared from aniline, pyrrole, thiophene or their derivatives which are very cheap compounds and also their preparation techniques are rather simple using chemical and electrochemical polymerizations. It is mentioned that these type of compounds have high conductivity (almost metallic conductivity); in addition, the conductivity can be changed by oxidation or reduction [2]. These valuable properties increase the popularity of conducting polymers and make them applicable in a variety of area. Sensors [21], light emitting diodes [22], solar cells [23], field effect transistors [24], and electrochromic devices [25] are some of the important industrial applications of conducting polymers.

1.6 Electrochromism

The reversible and visible change in transmittance or reflectance as a result of an applied voltage is called as electrochromism [26]. The increasing popularity of electrochromic materials in academia and industry can be explained by their dramatic spectroelectrochemical properties and their wide field of applications [27].

In order to characterize electrochromic materials different parameters can be used which are very useful to identify them and specify their usage area. Electrochromic contrast, coloration efficiency, switching speed, stability and optical memory are some of these parameters [28].

Electrochromic materials can be divided into three main types according to optical states. The changes in color between a colored and a transmissive state are the first case. Metal oxides, viologens, and polymers such as poly(3,4-ethylenedioxythiophene) (PEDOT) are important examples for this type. This type of electrochromic materials can be used for smart windows and optical shutters which are classified as absorption/transmission-type device applications. The second case is the color changes between the two colored states. Polythiophene which can be used for display-type applications is a good example of this type. Finally, the third case is the electrochromic materials having more than two color states which can also called as multicolored EC polymers. Conjugated polymers are good examples for this class [28].

1.6.1 Types of Electrochromic Materials

There are mainly three types of electrochromic materials; metal oxides, organic small molecules (viologens) and conducting polymers [29].

Transition-metal oxides with high band-gap such as tungsten oxide, WO_3 were widely studied over the past 30 years and these types of materials are the earliest electrochromic materials. Electrochromic properties for oxides of V, Mo, Nb, and Ti (cathodically coloring), and oxides of Ni, Co, and Ir (anodically coloring) were also studied [29]. Tungsten oxide is a transparent thin film in its neutral state and when it is electrochemically reduced the color of the thin film turned to blue. The following equation illustrates the electrochromic process of WO_3.

$$\underset{(transparent)}{WO_3} \quad + \quad xM^+ \quad + xe^- \rightarrow \quad \underset{(blue)}{M_xWO_3}$$

with $M^+ = H^+$, Li^+, Na^+, or K^+ [30].

Organic small molecules (viologens) are the another types of electrochromic materials. Diquaternization of 4,4'-bipyridyl yields 1,1'-disubstituted-4,4'-bipyridilium salts which is known as viologens. These small molecules have three redox states and between those the most stable one is the dication which is also colorless. Reduction of viologen dications generates radical cations which are intensely colored [31].

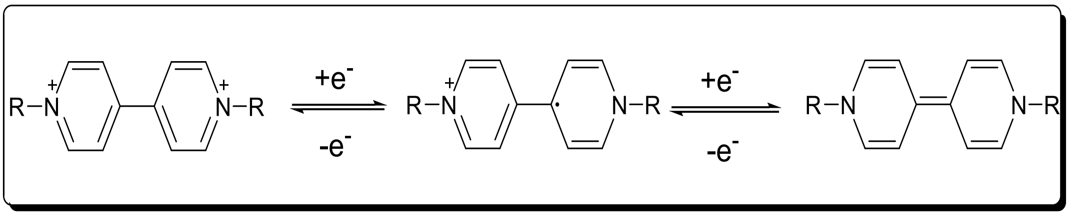

Figure 1. 10 The three common viologen redox states, dication, radical cation, neutral species.

Finally, as a third class conjugated polymers can be used as EC materials due to their fast switching times [32], high contrasts [33], processibility [34] and easy adjustment of electronic and optical properties via optical small structural changes [35]. Electrochromic materials can be used as an active layer for a variety of displays, smart windows, optical shutters, and mirror devices. This wide field of applications which are very important increased the popularity of conducting polymers [28].

Polythiophene (PTh), polypyrrole (PPy), and polyaniline (PANI) are widely studied examples of electrochromic materials which are conducting in thin film form but all of these polymers are insulating in neutral state and doping process makes them conducting by changing their optical and mechanical properties [30]. Electronic character of the conjugated polymers can be changed by reversible adding and removing ions on the polymer film (Figure 1.11). After doping process the changes in the energy gap (Eg) of the neutral polymer causes to have lower energy intraband transitions; polarons and bipolarons, which are also called as charge carriers which affect the conductivity [28].

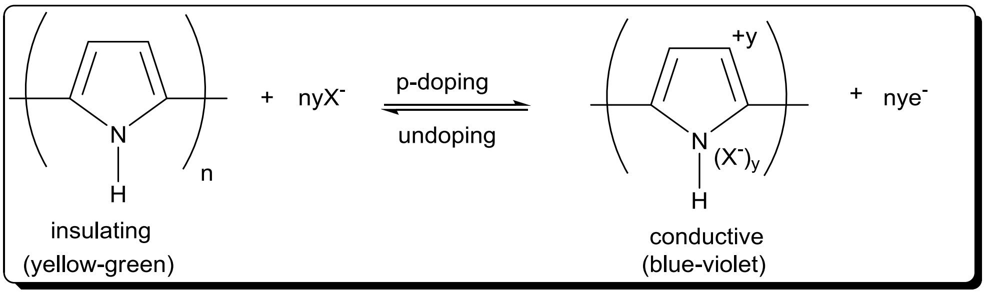

Figure 1. 11 The doped and undoped form of polypyrrole.

In order to explore doping process and its results spectroelectrochemical studies are commonly used. When the polymer is in its neutral state it has a single broad π- π^* transition and the energy difference can be showed with band gap (Eg), the difference between VB (Valance Band) and CB (Conduction Band). After oxidation formation of new absorption band is observed in the near-IR region which indicates the formation of radical cations (polarons). After further oxidation while the intensity of polaron bands and π- π* transition decrease, bipolaron bands are formed in the near-IR region. These changes alter the color of EC polymers [36].

1.6.2 Multicolor Electrochromic Polymers: Color Control

When we compare conjugated polymers as EC materials with others (inorganic compounds and viologens), the most important advantage is obviously their ease of structural modification by making small changes in the chemical structure. One can change the color of EC material in doped and undoped forms and synthesize multichromic polymers by the controlling band gap [37]. Copolymerization or homopolymerization can be used for band gap modification. In the literature modification of main chain and pendant groups are the widely used synthetic ways for adjusting band gap. EDOT is widely used as the donor group for that purpose. Figure 1.12 illustrates the examples of multicolor EC polymers synthesized by structural modification of monomers [28, 38].

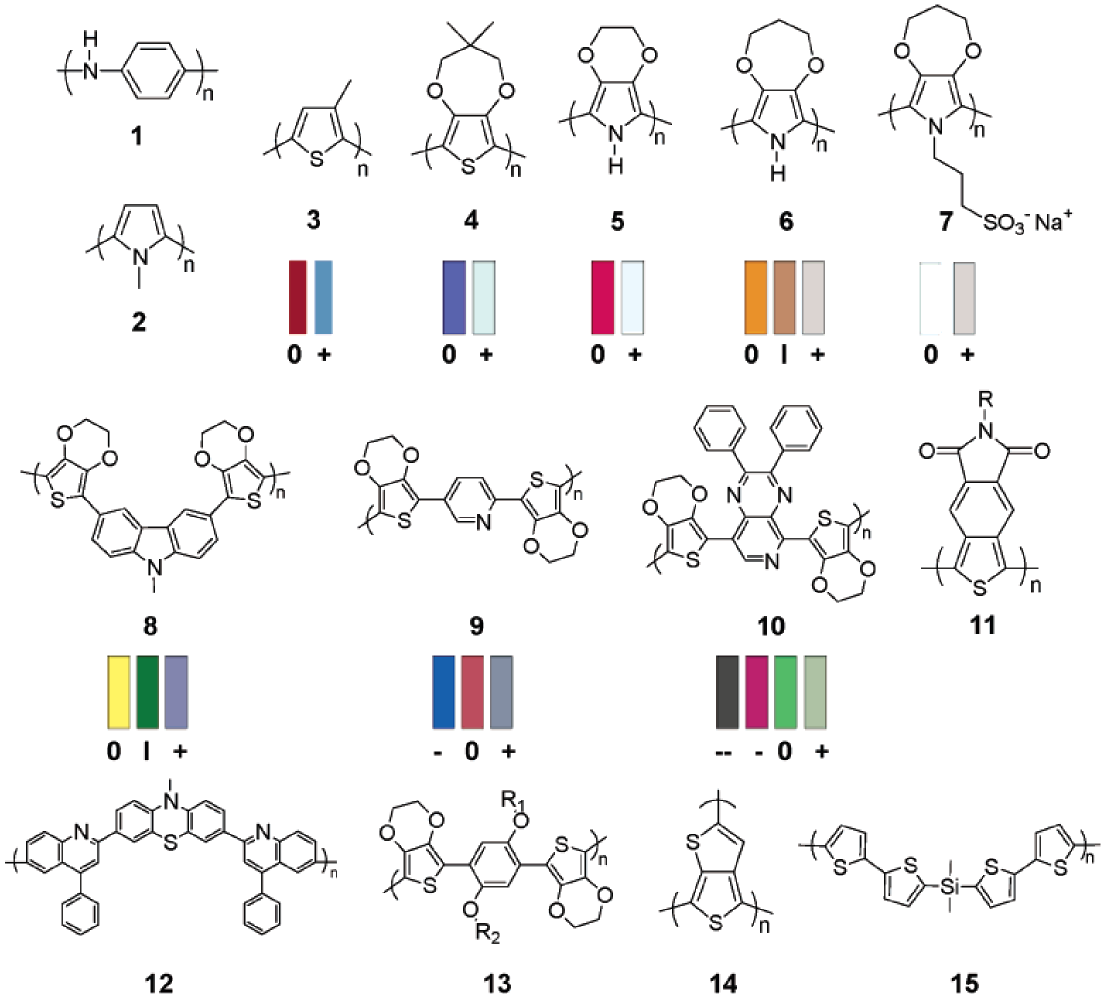

Figure 1. 12 Examples of multicolor EC polymers synthesized by structural modification. 0 = neutral; I= intermediate; + =oxidized; and-- = reduced

1.7 Low Band Gap Systems

Band gap does not only affect the color but also alter the conductivity of polymers. Low band gap polymers are an interesting class of materials which attract so many researchers in recent years due to their wide field of applications. Polymers which are transparent in doped state are very valuable materials and this rare property can also be satisfied by modification of band gap. As a result of this modification one can widen the application area of these polymers such as smart windows or electrodes.

In the literature, five basic methods were used to lower the band gap. Figure 1.13 shows these five methods for the alteration of band gap. Variation of bond length, increasing planarity of the systems, increasing stability of the polymer by using resonance, interchain effects and finally synthesizing donor-acceptor-donor type polymers are the methods for modification of band gap. Between them, the last one is the most advantageous and preferable one because this method minimize solubility problems and also provides variety in synthesis [39].

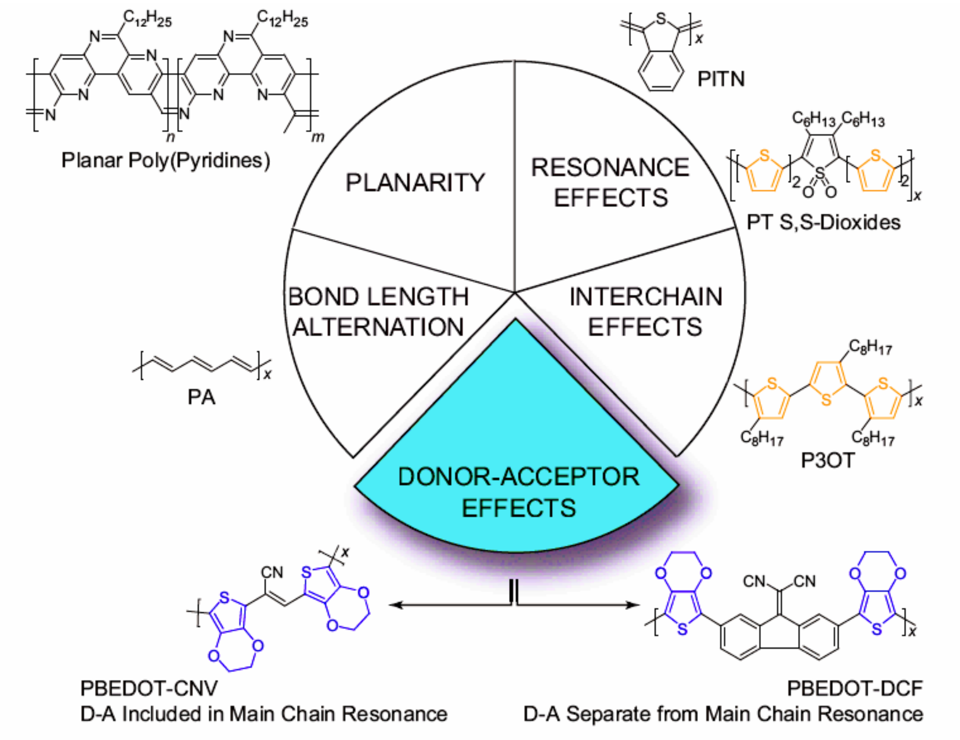

Figure 1. 13 Illustration of methods for the alteration of band gap

For the synthesis of D-A-D type polymers, type of donor and acceptor units and their proper match are also very important. A study of Thomas et al. illustrates this effect using cyanovinylene as the acceptor unit with five different donor units. Figure 1.14 shows the results of this study. When cyanovinylene is the acceptor unit, if we increase the electron donor ability of donor group, D-A match will be better and this proper match will lower band gap to 1.1 ev.[40].

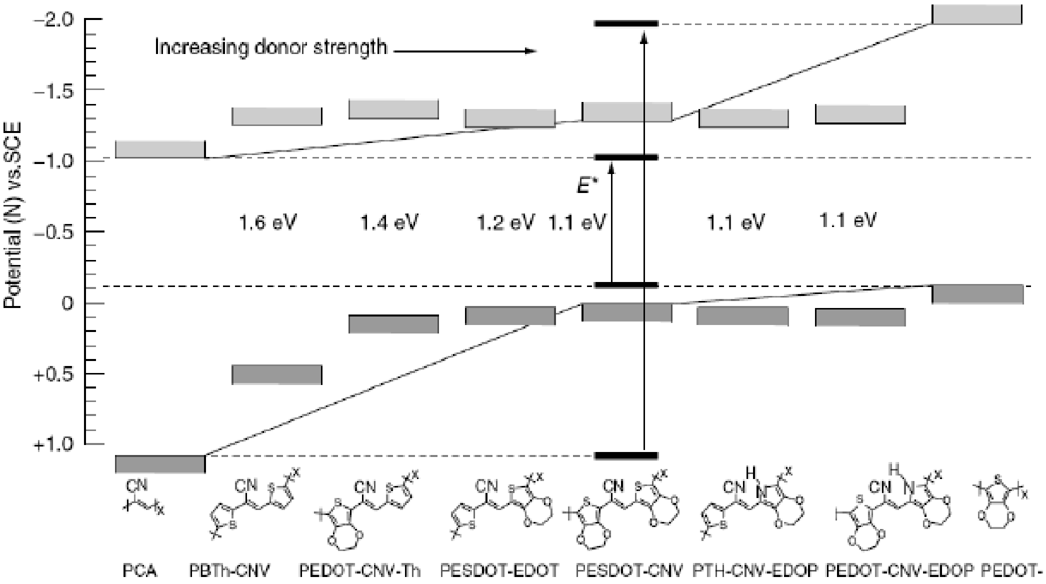

Figure 1. 14 VB and CB levels for cyanovinylene subsituted with different donor groups.

1.8 Color of Conducting Polymers and Importance of Green Polymeric Materials

The neutral state color of these conducting polymers is very important for device applications. Red, blue and green are the three main colors which were required for electrochromic devices. After these three were synthesized by mixing each of them all other colors can be acquired [41,42].

Most of the electrochromic polymers synthesized in the literature are red and blue colored and there was no neutral state green polymer until Sönmez and coworkers synthesized in 2004 [43]. Figure 1.15 illustates the structure of first neutral state green polymer synthesized by Gürsel Sönmez.

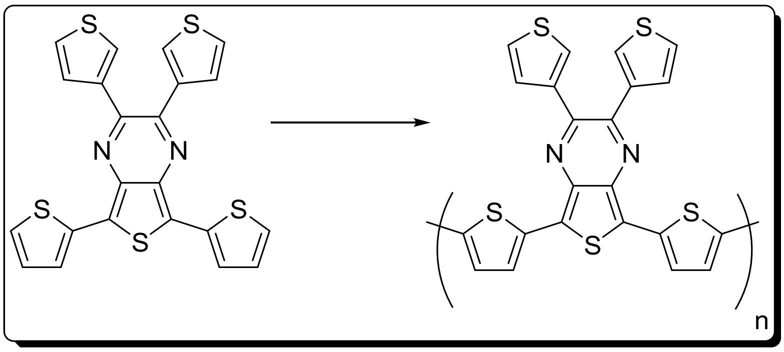

Figure 1. 15 Structure of the first neutral state green polymer.

The requirement for reflecting green color is having two concurrent absorption bands in the red and blue regions of the visible spectrum. In order to complete color space, transmissive oxidized state is another requirement. Unfortunately, the drawback of the first green polymer is its brown oxidized state. After that, Toppare Research Group synthesized neutral state gren polymer with highly transmissive oxidized oxidized state and also they enlarged the application area of conducting polymers by making them soluble [44].

Other neutral state green polymers with transmissive oxidized state synthesized by Toppare et al. and Reynolds et al. [45-48]. Figure 1.16 illustrates their structures.

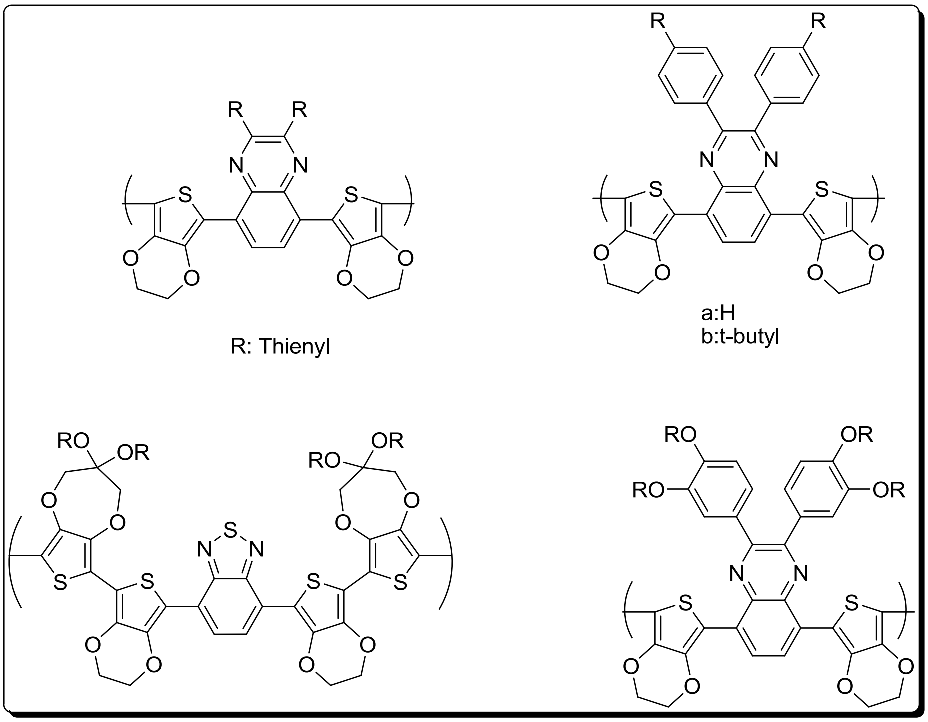

Figure 1. 16 Examples of gren polymeric materials with transmissive oxidized state.

1.9 Ferrocene Polymers

Ferrocene (Figure 1.17) is a metallocene, a type of organometallic compound consisting of two cyclopentadienyl rings bound on opposite sides of a central iron atom and forming an e-rich aromatic organometallic sandwich compound [49].

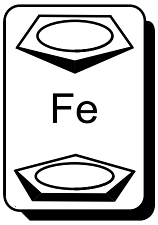

Figure 1. 17 Structure of ferrocene.

The importance and popularity of organometallic chemistry increased after the discovery of ferrocene. Altough 60 years passed after this important discovery, still new usage areas are found. One of these applications is using ferrocene in the polymer backbone to functionalize them and enlarge their usage area. There are mainly four reasons why ferrocene is preferred for functionalization of polymers. The electron rich character of ferrocene, its stability in both Fe(II) and Fe(III) oxidation states, steric effects and its easy substitution with a range of functional groups are the reasons mentioned above [50].

In addition, ferrocene is widely used in the backbone of conducting polymers. Conducting polymers functionalized by metals are another type of useful and fascinating materials. These type of materials show both redox properties of the conducting polymer and also metals [51]. In the literature Pt [52], Rh [53], Au [54] and Ru [55] functionalized conducting polymers were also synthesized but most of the studies focused on ferrocene functionilized conducting polymers.

Conducting polymers containing metals can be splitted into three types. *These are types I, II and III named as tethered, coupled and incorporated respectively* [51]. For type I polymers metal attached to the polymer backbone by a linker group. Alkyl groups can be used as a linker for this case. For type II polymers metal directly connected to the conjugated part so the effect of metal on polymer backbone or vica versa increase. Finally for type III polymers the maximum effect of metal on conjugated part is observed due to metal incorporation into the polymer backbone [51]. Figure 1.18 illustrates the structures of metal containing conducting polymers.

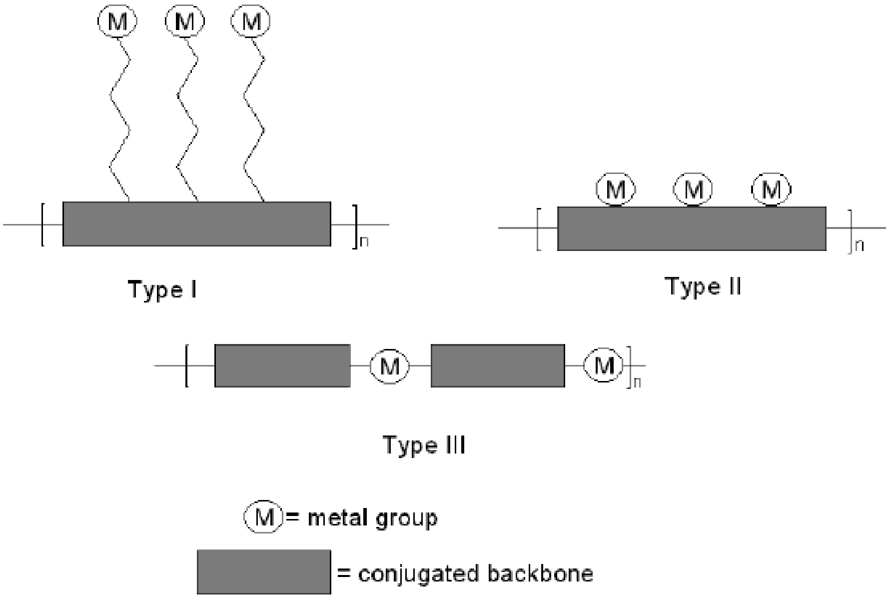

Figure 1. 18 Schematic representation of three types of metal containing conducting polymers.

Wide field of applications of ferrocene functionalized conducting polymers also increase their popularity. Sensors [56, 57], electro active Langmuir/Blodgett films [58], free-standing redox-active films [59] are the important application of these materials.

In the literature, “ferrocene functionalized poly (3, 4-ethylenedioxythiophene) (PEDOT) conductive polymer was prepared via copper-catalyzed azide–alkyne cycloaddition reaction and its electrochemical experiments revealed that the ferrocene clicked PEDOT films have fast electron transfer ability. The spectroelectrochemical studies show that the conducting polymer can switch from opaque purple to red then blue with a contract of 20% in oxidized state and switching time around 600 ms” [60].

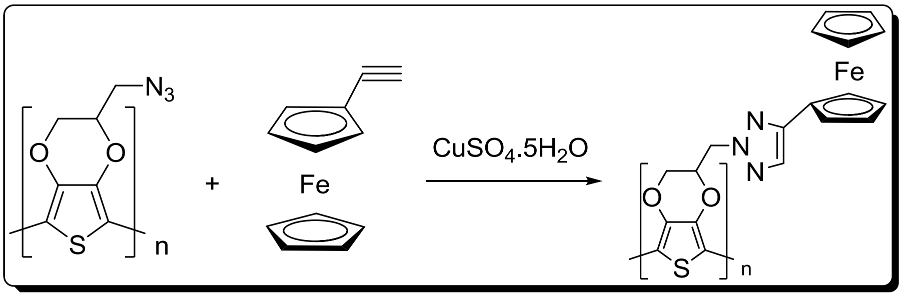

Figure 1. 19 Synthetic route to Ferrocene clicked poly(3,4-ethylenedioxythiophene).

Oligothienylferrocene complexes were also synthesized in the literature to illustrate the effect of ferrocene when placed on the backbone of the polymer. 1,1-Bis(5-(2,2-bithienyl))ferrocene and 1,1-bis(5-(2,2:5,2-terthienyl)) ferrocene were synthesized and their electrochemical characterization was performed. Results of this study state that 'Oxidation of the ferrocene group to ferrocenium in both the monomers and in the electropolymerized films results in the appearance of a low-energy charge transfer transition' [61].

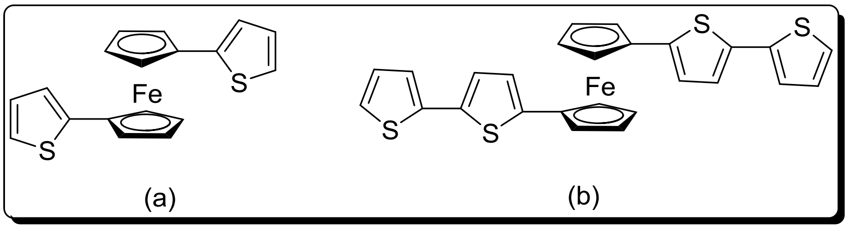

Figure 1. 20 Structures of a) 1,1-bis(5-(2,2-bithienyl))ferrocene and b) 1,1-bis(5-(2,2:5,2-terthienyl)) ferrocene.

1.10 Aim of This Work

The aim of this work is to synthesize three new donor acceptor donor type monomers; 5,8-bis(2,3-dihydrothieno[3,4 b][1,4]dioxin-5-yl)-2-(naphthalen-2-yl)-3-ferrocenyl-4a,8a-dihydroquinoxaline (DEFNQ), 5,8-bis(2,3-dihydrothieno[3,4-b][1,4]dioxin-5-yl)-2-(phenyl)-3 ferrocenylquinoxaline (DEFPQ) and 5,8-bis(2,3-dihydrothieno[3,4-b][1,4]dioxin-5-yl)-2,3-di(naphthalen-2-yl)quinoxaline (DEDNQ) and electrochemically polymerize them. Electron defficient quinoxaline unit was used as an acceptor unit and EDOT was used as a donor group during synthesis. The main purpose of synthesizing these monomers is to investigate effect of ferrocene subsituent on spectroelectrochemical behaviors of these polymers.

CHAPTER 2

EXPERIMENTAL

2.1 Materials and Methods

All chemicals and reagents were obtained from commercial sources and used without further purification. Ferrocene Carboxaldehyde (Aldrich), β-Naphtaldehyde (Aldrich), manganese dioxide (MnO_2), 3,4-ethylenedioxythiophene (EDOT) (Aldrich), benzothiadiazole (Aldrich), sodium borohydride ($NaBH_4$) (Aldrich), potassium cyanide (KCN) (Aldrich), bromine (Br_2) (Aldrich), dichloromethane (DCM) (Merck), chloroform ($CHCl_3$) (Merck), *p*-Toluenesulfonic acid (PTSA) (Aldrich) were used as received. Benzaldehyde (Aldrich) was distilled before use. Tetrahydrofuran (THF) (Across) was dried with sodium and benzophenone before use.

2.2 Equipment

VoltaLab PST050 and Solartron 1285 potentiostats were used for cyclic voltammetry studies in order to supply a constant potential. One-compartment cell was used for electrolyses and all of the measurements were performed in an open air medium. The working electrode was ITO, counter electrode was platinum (Pt) and the reference electrode was silver (Ag) wire. For the spectroelectrochemistry studies a Varian Cary 5000 UV-Vis spectrophotometer was used. Bruker-Instrument-NMR Spectrometer (DPX-400) was used to record ^{1}H-NMR and ^{13}C-NMR spectra of the monomers,

$CDCl_3$ was chosen as the solvent and chemical shifts (δ) were given in ppm relative to tetramethylsilane as the internal standard.

2.3 Procedure, Synthesis

2.3.1 Synthesis of 2-Hydroxy-2-(naphthalen-2-yl)-1-ferrocenylethanone (3)

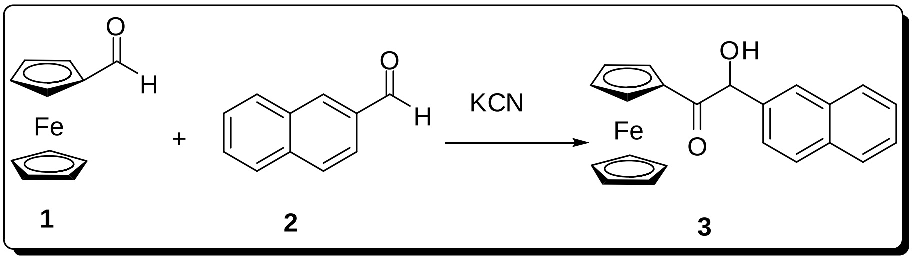

Figure 2. 1 Synthesis of 2-Hydroxy-2-(naphthalen-2-yl)-1-ferrocenylethanone (**3**)

Synthesis of 2-Hydroxy-2-(naphthalen-2-yl)-1-ferrocenylethanone was performed according to methodology described in the literature [62]. Ferrocene carboxaldehyde (0,5 g, 0.002 mol), β-naphthaldehyde (0.41 g, 0.002 mol), and KCN (0.082 g, 0,0015 mol) were dissolved in 1.5 mL H_2O and 3 mL ethanol, then refluxed for 3 h. The mixture was cooled to 0 °C and concentrated on the rotary evaporator. The residue was subjected to column chromatography (silica gel, hexane: EtOH, 15:1). Compound **3** was obtained as an orange solid in 77.0% yield. ^1H NMR (400 MHz, $CDCl_3$) δ 7.81–7.71 (m, 4H), 7.42–7.38 (m, 2H), 7.37–7.34 (m, 1H), 5.57 (d, *J* = 5.7 Hz, 1H), 4.81 (dd, *J* = 2.6, 1.3 Hz, 1H), 4.61 (dd, *J* = 2.6, 1.3 Hz, 1H), 4.58 (d, *J* = 6.0 Hz, 1H), 4.45 (td, *J* = 2.6, 1.2 Hz, 1H), 4.37 (dt, *J* = 3.9, 1.9 Hz, 1H), 4.00 (s, *J* = 4.5 Hz, 5H). ^{13}C NMR (101 MHz, $CDCl_3$) δ 203, 137.5, 137.4, 133.3, 133.2, 128.9, 128.1, 127.7, 127.4, 126.4, 124.9, 73.0, 73.0, 70.4, 70.2, 69.8.

2.3.2 Synthesis of 1-ferrocenyl-2-naphthylethanedione (4)

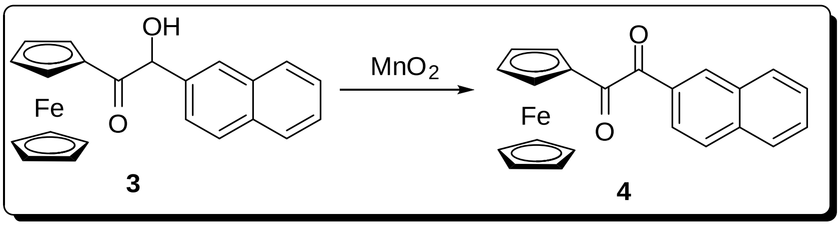

Figure 2. 2 Synthetic route for 1-ferrocenyl-2-naphthylethanedione (**4**)

Synthesis of 1-ferrocenyl-2-naphthylethanedione was performed according to methodology described in the literature [62]. 2-Hydroxy-2-(naphthalen-2-yl)-1-ferrocenylethanone (129 mg, 0.35 mmol) was dissolved in $CHCl_3$ (5 mL) and refluxed. MnO_2 and charcoal (activated in the oven) were added to the mixture in catalytic amount, then the mixture was stirred under reflux for 2 days. The mixture was concentrated and subjected to column chromotography (silica gel, hexane: EtOH, 10:1) to get 4 (95 mg, , 74%) as a red solid. ^{1}H NMR (400 MHz, CDCl3) δ 8.48 (s, 1H), 8.04 (dd, *J* = 8.6, 1.7 Hz, 1H), 7.92–7.77 (m, 3H), 7.64–7.42 (m, 2H), 4.96–4.76 (m, 2H), 4.67–4.54 (m, 2H), 4.21 (s, 5H). ^{13}C NMR (101 MHz, $CDCl_3$) 199.3, 193.5, 136.8, 133.6, 133.1, 131.0, 130.5, 129.9, 129.5, 128.5, 127.7, 124.7, 75.4, 74.6, 71.1, 71.1.

2.3.3 Synthesis of 1-ferrocenyl-2-phenylethanedione (7)

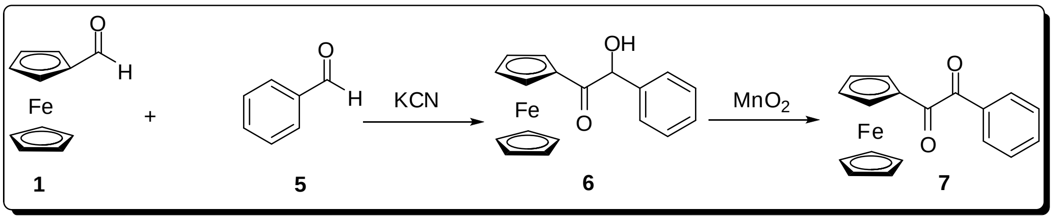

Figure 2. 3 Synthetic route for 1-ferrocenyl-2-phenylethanedione (**7**)

Synthesis of 1-ferrocenyl-2-phenylethanedione was performed according to methodology described in the literature [62] and the procedure is given in the previous part. Compound **6** was synthesized by benzoin condensation with 60% yield. Oxidation of **6** with MnO_2 gave desired compound (1-ferrocenyl-2-phenylethanedione) as a puple solid with 72% yield. ^{1}H NMR (400 MHz, CDCl3) δ 8.02–7.93 (m, 2H), 7.54 (t, J = 7.4 Hz, 1H), 7.43 (t, *J* = 7.6 Hz, 2H), 4.82–4.72 (m, 2H), 4.60–4.50 (m, 2H), 4.18 (s, 5H). ^{13}C NMR (101 MHz, $CDCl_3$) δ 199.2, 191.5, 134.0, 133.5, 129.9, 128.6, 77.1, 76.8, 76.5, 73.4, 70.4.

2.3.4 Synthesis of 1,2-di(naphthalen-2-yl)ethane-1,2-dione (9)

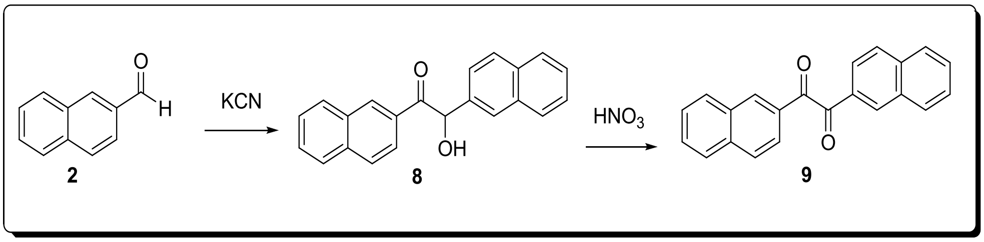

Figure 2. 4 Synthetic route for 1,2-di(naphthalen-2-yl)ethane-1,2-dione **(9)**

Synthesis of 1,2-di(naphthalen-2-yl)ethane-1,2-dione was performed according to methodology described in the literature [62] and the procedure given in the previous part. Compound **8** was synthesized by benzoin condensation in 65% yield. Oxidation of **8** with HNO_3 gave desired compound (1,2-di(naphthalen-2-yl)ethane-1,2-dione) as a yellow solid in 88% yield . ^{1}H NMR (400 MHz, CDCl3) δ 9.18 (d, *J* = 12.7 Hz, 1H), 8.70 (d, *J* = 9.4 Hz, 1H), 8.59–8.52 (m, 1H), 8.40–8.03 (m, 9H), 7.73–7.58 (m, 2H). ^{13}C NMR (101 MHz, $CDCl_3$) 134.3, 130.7, 129.9, 129.8, 129.6, 127.9, 125.4, 123.8, 123.7, 123.6, 121.7.

2.3.5 Synthesis of 4,7-Dibromo-2.1.3-benzothiadiazole (11)

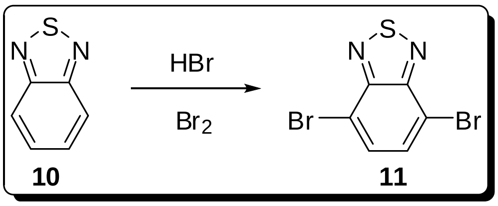

Figure 2. 5 Synthetic route for 4,7-Dibromo-2.1.3-benzothiadiazole (**11**)

Synthesis of 4,7-dibromo-2.1.3-benzothiadiazole was performed according to methodology described in the literature [63]. Benzothiadiazole (500 mg, 3.67 mmol) and HBr (9 mL) were mixed in a flask and a solution containing Br_2 (0.4 mL) in HBr (4 mL) was added dropwise to the mixture very slowly. After Br_2 addition was completed, the solution was refluxed for 6 h. and cooled to room temperature. Excess Br_2 was consumed with saturated solution of $NaHSO_3$. The filtered solution yielded the desired dibrominated product **11** in 90% yield (960 mg, 3.3 mmol). ^1H NMR (400 MHz, $CDCl_3$) δ 7.66 (s, 2H). ^{13}C NMR (101 MHz, $CDCl_3$) δ 152.9, 132.3, 113.9.

2.3.6 Synthesis of 3,6-dibromo-1,2-phenylenediamine (12)

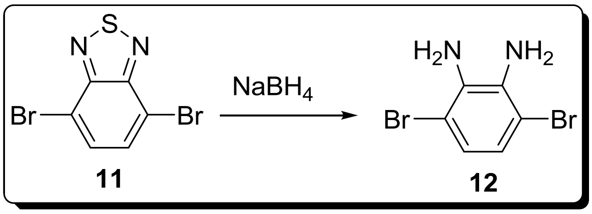

Figure 2. 6 Synthetic route for 3,6-dibromo-1,2-phenylenediamine (**12**)

Synthesis of 3,6-dibromo-1,2-phenylenediamine was performed according to methodology described in the literature [64]. 4, 7-Dibromo-2.1.3-benzothiadiazole (300 mg, 1.03 mmol) was dissolved in EtOH (25 mL). To this mixture, sodium borohydride (1.5 g, 0.04 mol) was added in small portions at 0 ^{o}C, and the mixture was stirred for 24 h at room temperature. The solvent was evaporated completely, and the extraction was performed firstly with ether and water, secondly with ether and brine. Removing all of the solvent yielded 3,6-dibromo-1,2-phenylenediamine (**12**) (234 mg, 0.88 mmol) as a pale yellow solid in 86% yield. ^{1}H NMR (400 MHz, $CDCl_3$) δ 6.78 (s, 2H), 3.82 (s, 4H). ^{13}C NMR (101 MHz, $CDCl_3$) δ 133.5, 123.2, 109.5.

2.3.7 Synthesis of tributl(2,3-dihydrothieno[3,4-b][1,4]dioxin-5-yl)stannane (14)

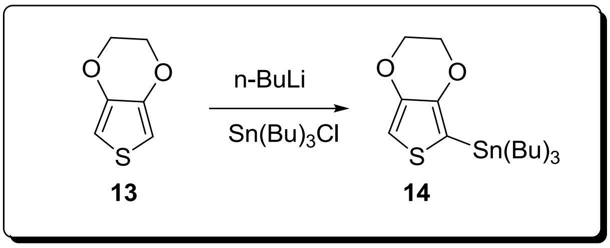

Figure 2. 7 Synthetic route for tributyl(2,3-dihydrothieno[3,4-b][1,4]dioxin-5-yl)stannane (**14**)

Tributyl(2,3-dihydrothieno[3,4-b][1,4]dioxin-5-yl)stannane was synthesized according to a methodology described in the literature [65]. EDOT (2 g, 14 mmol) was dissolved in THF (40 mL). After the solution was cooled to -78^{o}C, n-BuLi (8.7mL, 14 mmol) was added very slowly and then tributyltin chloride (4.6 g, 14 mmol) was added at -78 ^{o}C. The mixture was stirred at room temperature for 24 h. Water (50 mL) was added to the mixture to finish the reaction. Extraction was performed with DCM and concentrated to get desired product **14**. ^{1}H NMR ($CDCl_3$) δ 6.56 (s,1H), 4.16 (s, 4H), 1.61-1.49 (m, 6H), 1.39-1.22 (m, 6H), 1.09(m, 9H), 0.9

(m, 6H). ^{13}C NMR ($CDCl_3$) δ 147.88, 142.65, 109.8, 105.99, 64.86, 64.80, 29.08, 27.40, 13.76, 10.72.

2.3.8 Synthesis of 5,8-dibromo-2-(naphthalen-2-yl)-3-ferrocenyl-4a,8a-dihydroquinoxaline (15)

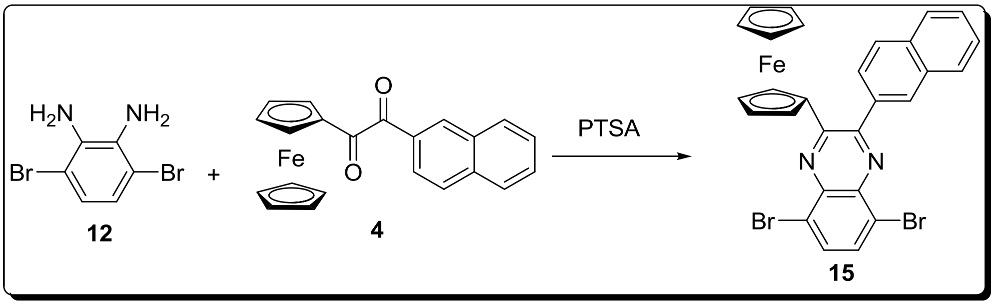

Figure 2. 8 Synthetic route for 5,8-dibromo-2-(naphthalen-2-yl)-3-ferrocenyl-4a,8a-dihydroquinoxaline (**15**)

A solution of 3,6-dibromo-1,2-phenylenediamine (168.6 mg,0.64 mmol) and 1-ferrocenyl-2-naphthylethanedione (231 mg, 0.63 mmol) in EtOH (40.6 mL) was refluxed overnight with a catalytic amount of *p*-toluene sulfonic acid (PTSA). The mixture was cooled to 0 °C. The precipitate was isolated by filtration and washed with EtOH several times to afford the desired compound in 89 % yield (140 mg, 0.279 mmol). ^{1}H NMR ($CDCl_3$) δ 8.15 (s, 1H), 7.87–7.76 (m, J = 14.4 and 7.1 Hz, 5H), 7.63 (dd, J = 8.5 and 1.6 Hz, 1H), 7.51 – 7.45 (m, 2H), 4.60 – 4.57 (m, 2H), 4.28–4.25 (m, 2H), 3.93 (s, 5H). ^{13}C NMR ($CDCl_3$) δ 156.05, 153.75, 139.70, 138.24, 135.95, 133.66, 133.00, 132.94, 131.96, 129.58, 128.71, 127.81, 127.76, 127.07, 127.04, 126.49, 123.72, 123.14, 71.72, 70.52, 70.23.

2.3.9 Synthesis of 5,8-bis(2,3-dihydrothieno[3,4-b][1,4]dioxin-5-yl)-2-(naphthalen-2-yl)-3-ferrocenyl-4a,8a-dihydroquinoxaline (M1)

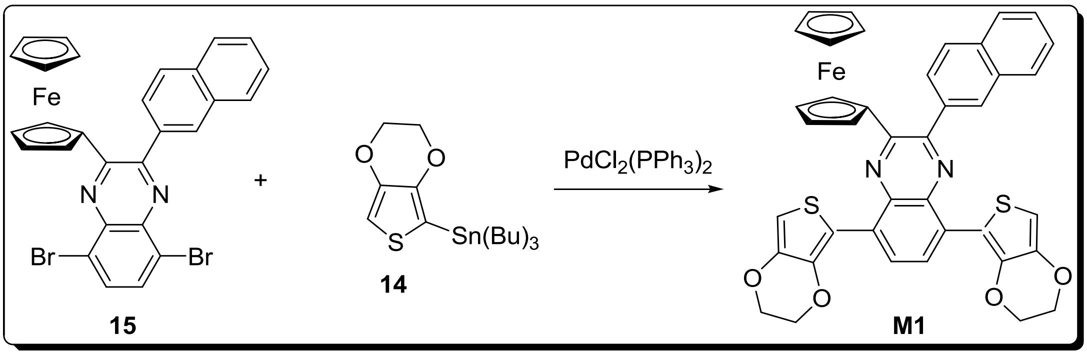

Figure 2. 9 Synthetic route for 5,8-bis(2,3-dihydrothieno[3,4-b][1,4]dioxin-5-yl)-2-(naphthalen-2-yl)-3-ferrocenyl-4a,8a-dihydroquinoxaline (**M1**)

5,8-Dibromo-2-(naphthalen-2-yl)-3-ferrocenyl-4a,8a-dihydroquinoxaline (50 mg, 0.0836 mmol) and tributyl (2,3-dihydrothieno[3,4-b][1,4]dioxin-5-yl)stannane (478.8 mg, 0.753mmol) were dissolved in dry THF (25 mL). The solution was purged with argon for 30 min. and $PdCl_2(PPh_3)_2$ was added under argon atmosphere. The mixture was stirred at 100 ^{o}C under argon atmosphere for 15 h, cooled and concentrated on the rotary evaporator. The residue was subjected to column chromatography (silica gel, $CHCl_3$: hexane, 2:1) to afford a red solid in 88.0% yield (53 mg, 0.074 mmol). ^{1}H NMR ($CDCl_3$) δ 8.63 – 8.49 (m, 2H), 8.23 (s, 1H), 7.89–7.83 (m, 3H), 7.75 (dd, *J* = 8.5 and 1.6 Hz, 1H), 7.52–7.44 (m, 2H), 6.61 (s, 1H), 6.42 (s, 1H), 4.76–4.70 (m, 2H), 4.40–4.35 (m, 2H), 4.34–4.30 (m, 2H), 4.30–4.26 (m, 2H), 4.25 (dd, *J* = 4.9 and 2.9 Hz, 2H), 4.24–4.19 (m, 2H), 3.91 (s, 5H). ^{13}C NMR ($CDCl_3$) δ 151.99, 150.10, 141.49, 141.32, 140.32, 140.23, 137.48, 136.90, 135.95, 133.39, 133.10, 129.63, 128.90, 128.66, 128.01, 127.81, 127.71, 127.67, 127.56, 127.01, 126.67, 126.26, 113.47, 103.10, 102.78, 82.32, 77.21, 71.87, 70.06, 70.04, 65.01, 64.96, 64.39, 64.35.

2.3.10 Synthesis of 5,8-dibromo-2-phenyl-3-ferrocenylquinoxaline (16)

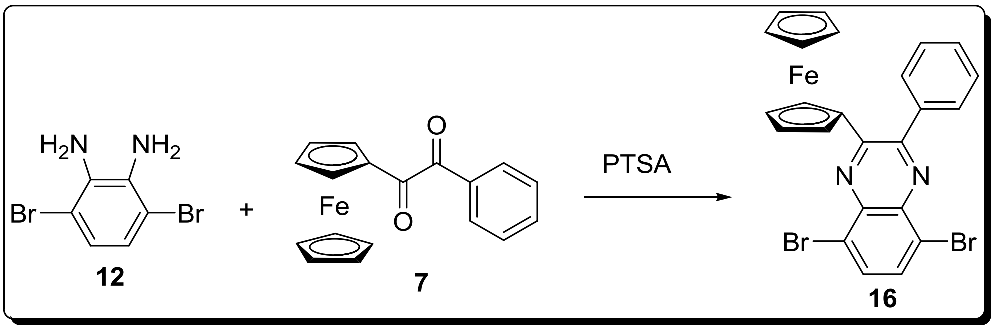

Figure 2. 10 Synthetic route for 5,8-dibromo-2-phenyl-3-ferrocenylquinoxaline (**16**)

A solution of 3,6-dibromo-1,2-phenylenediamine (166 mg,0.63 mmol) and 1-ferrocenyl-2-phenylethanedione (200 mg, 0.63 mmol) in EtOH (50 mL) was refluxed overnight with a catalytic amount of *p*-toluene sulfonic acid (PTSA). The mixture was cooled to 0 °C and concentrated on the rotary evaporator. The residue was subjected to column chromatography (silica gel, hexane:EtOH, 10:1). Compound **16** was obtained as a purple solid in 73.0% yield (249 mg, 0.45 mmol). ^{1}H NMR (400 MHz, $CDCl_3$) δ 7.79 (d, 1H), 7.76 (d, 1H), 7.59–7.55 (m, 2H), 7.41–7.35 (m, 3H), 4.57–4.53 (m, 2H), 4.28–4.25 (m, 2H), 3.91 (s, 5H). ^{13}C NMR (101 MHz, $CDCl_3$) δ 156.3, 153.73, 139.7, 138.7, 138.3, 132.7, 131.8, 129.8, 129.3, 128.1, 123.8, 123.1, 96.1, 82.1, 71.6, 70.2, 70.2.

2.3.11 Synthesis of 5,8-bis(2,3-dihydrothieno[3,4-b][1,4]dioxin-5-yl)-2-(phenyll)-3-ferrocenylquinoxaline (M2)

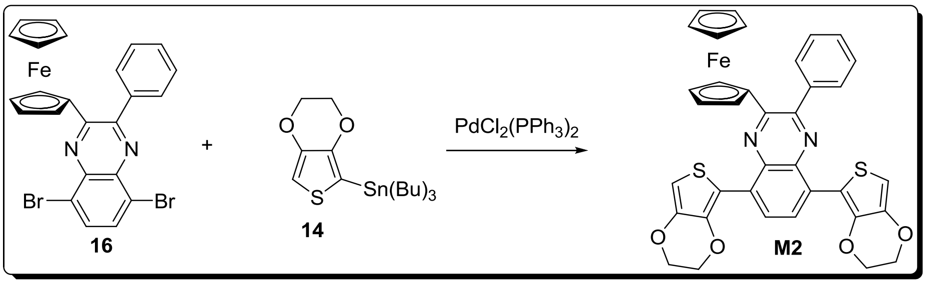

Figure 2. 11 Synthetic route for 5,8-bis(2,3-dihydrothieno[3,4-b][1,4]dioxin-5-yl)-2-(phenyll)-3-ferrocenylquinoxaline (**M2**)

5,8-Dibromo-2-phenyl-3-ferrocenylquinoxaline (240 mg, 0.438 mmol) and tributyl (2,3-dihydrothieno[3,4-b][1,4]dioxin-5-yl)stannane (1.393 g, 2.19 mmol) were dissolved in dry THF (100 mL). The solution was purged with argon for 30 min. and $PdCl_2(PPh_3)_2$ was added under argon atmosphere. The mixture was stirred at 100 ^oC under argon atmosphere for 18 h, cooled and concentrated on the rotary evaporator. The residue was subjected to column chromatography (silica gel, $CHCl_3$: hexane, 2:1) to afford a red solid in 68.0% yield (198 mg, 0.295 mmol). ^1H NMR (400 MHz, $CDCl_3$) δ 8.63 (d, 1H), 8.55 (d, 1H), 7.78–7.70 (m, 2H), 7.46 (dd, *J* = 8.0, 3.0 Hz, 3H), 6.65 (s, 1H), 6.49 (s, 1H), 4.79–4.76 (m, 2H), 4.41 (dd, *J* = 5.2, 2.4 Hz, 2H), 4.37 (dd, *J* = 5.2, 2.4 Hz, 2H), 4.34–4.32 (m, 2H), 4.31 (dd, *J* = 3.7 Hz, 2H), 4.27 (dd, *J* = 4.1 Hz, 2H), 3.95 (s, 5H). ^{13}C NMR (101 MHz, $CDCl_3$) δ 151,9, 150,1, 141.4, 141.3, 140.3, 140.2, 137.5, 136.9, 135.9, 133.3, 133.1, 129.6, 128.9, 128.6, 128.0, 127.8, 127.7, 127.6, 127.5, 127.0, 126.6, 126.2, 113.4, 103.1, 102.7, 82.3, 71.8, 70.0, 64.9, 64.3.

2.3.12 Synthesis of 5,8-dibromo-2,3-di(naphthalen-2-yl)quinoxaline

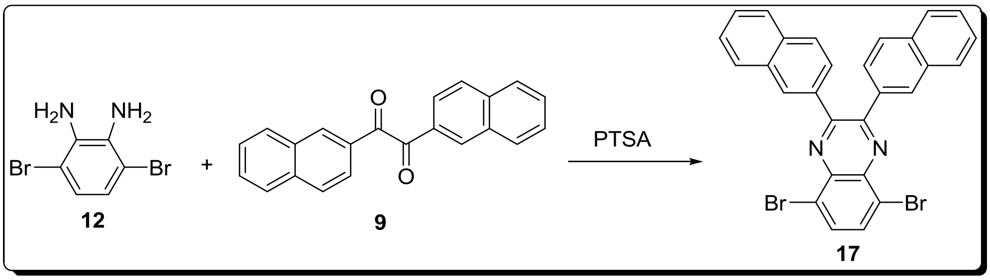

Figure 2. 12 Synthetic route for 5,8-dibromo-2,3-di(naphthalen-2-yl)quinoxaline

A solution of 3,6-dibromo-1,2-phenylenediamine (86 mg,0.33 mmol) and 1,2-di(naphthalen-2-yl)ethane-1,2-dione (100 mg, 0.322mmol) in EtOH (25 mL) was refluxed overnight with a catalytic amount of *p*-toluene sulfonic acid (PTSA). The mixture was cooled to 0 °C. The precipitate was isolated by filtration and washed with EtOH several times then the residue was subjected to column chromatography (silica gel, $CHCl_3$: hexane, 1:1) to get the product as a yellow solid in 67 % yield (116 mg, 0.214 mmol). ^{1}H NMR (400 MHz, $CDCl_3$) δ 8.96–8.81 (m, 1H), 8.55–7.99 (m, 7H), 7.95 (d, 2H), 7.92–7.65 (m, 4H), 7.56–7.46 (m, 2H). 13C NMR (101 MHz, CDCl3) δ 152.8, 147.0, 135.4, 134.5, 133.9, 130.8, 130.3, 129.1, 128.9, 128.4, 126.2, 125.4, 125.0, 124.8.

2.3.13 Synthesis of 5,8-bis(2,3-dihydrothieno[3,4-b][1,4]dioxin-5-yl)-2,3-di(naphthalen-2-yl)quinoxaline (M3)

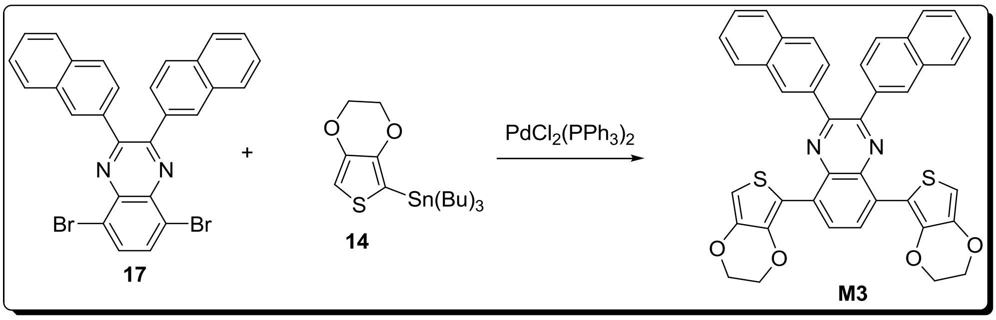

Figure 2. 13 Synthetic route for 5,8-bis(2,3-dihydrothieno[3,4-b][1,4]dioxin-5-yl)-2,3-di(naphthalen-2-yl)quinoxaline (**M3**)

5,8-Dibromo-2,3-di(naphthalen-2-yl)quinoxaline (400 mg, 0.74 mmol) and tributyl (2,3-dihydrothieno[3,4-b][1,4]dioxin-5-yl)stannane (2.35 g, 3,7 mmol) were dissolved in dry THF (130 mL). The solution was purged with argon for 30 min. and $PdCl_2(PPh_3)_2$ was added under argon atmosphere. The mixture was stirred at 100 ^oC under argon atmosphere for 18 h, cooled and concentrated on the rotary evaporator. The residue was subjected to column chromatography (silica gel, $CHCl_3$: hexane, 2:1) to afford a red solid in 65.0 % yield (318.5 mg, 0.48 mmol). ^1H NMR (400 MHz, $CDCl_3$) δ 9.23–8.44 (m, 6H), 8.38–7.60 (m, 8H), 7.59–7.39 (m, 2H), 6.51 (s, 2H), 4.35 (dd, *J=3.55*, 4H), 4.25 (dd, *J=3.78*, 4H). ^{13}C NMR (101 MHz, $CDCl_3$) δ 148.9, 146.4, 141.4, 140.6, 139.1, 137.4, 135.4, 134.3, 131.1, 129.01, 128.9, 125.9, 125.1, 124.9, 124.3, 123.2, 112.1, 103.4, 65.0, 64.3.

CHAPTER 3

RESULTS AND DISCUSSION

3.1 Electrochemical and Electrochromic Properties of Quinoxaline Derivative Polymers

3.1.1 Electrochemical and Electrochromic Properties of PDEFNQ (P1)

3.1.1.1 Electrochemistry of DEFNQ (M1)

The potentiodynamic electropolymerization for **M1** was performed in 0.1 M tetrabutylammonium hexafluorophosphate (TBAPF$_6$) and solvent system was chosen as acetonitrile (ACN)/ dichloromethane (DCM) (5:95, v:v) mixture. Indium tin oxide coated glass slides (ITO) were used as the working electrode whereto polymer films are produced.

Figure 3.1a illustates single scan voltammograms of Fc, and electron defficient acceptor unit of the monomer. Figure 3.1b represents the first run of electropolymerization of DEFNQ (**M1**). The reversible oxidation/reduction peaks of Fc (ferrocene) were recorded at 0.78 V and 0.17 V respectively, versus Ag wire pseudo reference electrode. When Fc attached to the quinoxaline unit, the oxidation potential of Fc was shifted to a slightly higher potential since quinoxaline is an electron defficient group.

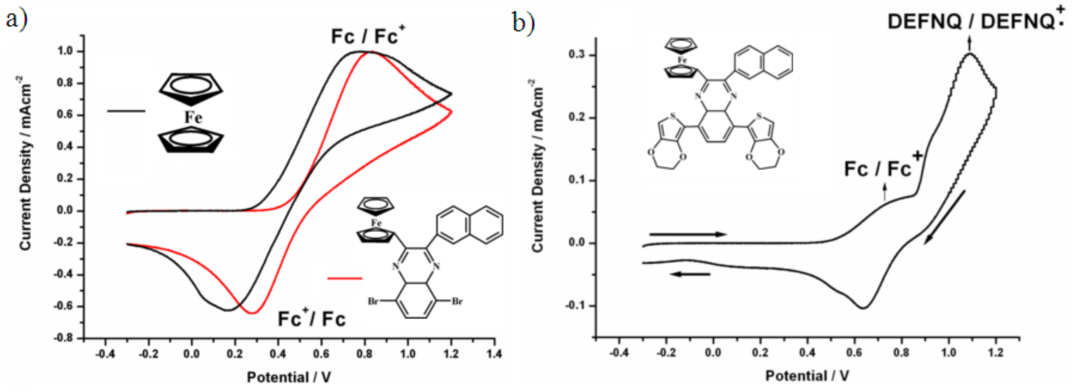

Figure 3. 1 Single scan voltammograms of a) Fc — , acceptor unit — in ACN and b) the first run of electropolymerization of **M1** in a DCM/ACN (5:95,v:v)/ TBAPF6 solvent-electrolyte couple.

Figure 3.1b shows the first run of electropolymerization, first peak at 0.72 V belongs to ferrocene oxidation. Reversible monomer oxidation/reduction peaks were appeared at 1,1 V and 0.63 V. As a result of this reduction polymer chains started to form which generates electrode passivation and hence Fc reduction peak can not be seen.

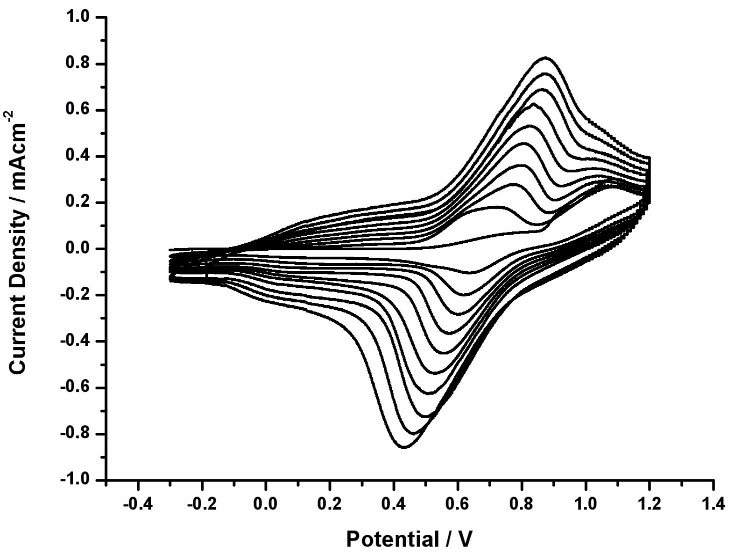

Figure 3. 2 Multiple scan voltammogram for polymerization of **M1** in DCM/ACN/ TBAPF6 solution.

Reversible anodic and cathodic peaks at 0.82 V and at 0.45 V with increasing number of cycles shows the formation of **P1** (Figure 3.2).

Resulting polymer was subjected to CV in order to investigate the n-type doping property of the **P1**. **P1** showed both p- and n-doping properties which were proven by a reversible redox couple at -1.7 V and -1.35 V (Figure 3.3). Although almost all conjugated polymers have a tendency to be p doped, only handful of them reveal ambipolar characteristics which have numerous applications such as; light emitting diodes and ambipolar transistors [66]. It is striking to notice that full cycles (p and n doping) for P1 were recorded with consecutive cycles under ambient conditions which indicates the stability of doped states [67].

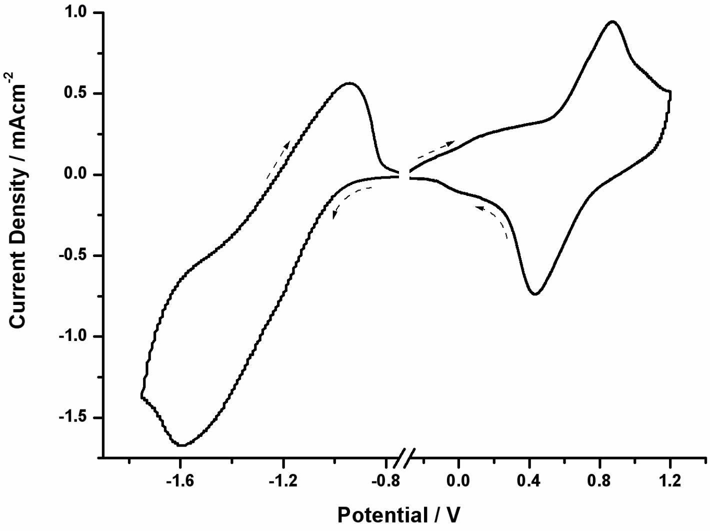

Figure 3. 3 Single scan voltammogram of **P1** upon both p and n-type doping.

The anodic and cathodic peaks of PDEFNQ were proportional to each other even at different scan rates which is an indication of a well adhered polymer film and a non diffusion controlled charge transfer process (Figure 3.4) [68]

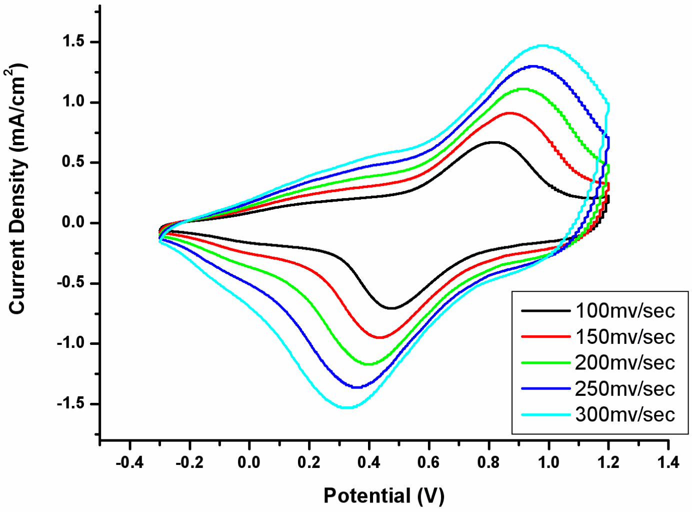

Figure 3. 4 Scan rate dependence of P1 films at 100, 150, 200, 250, and 300 mV/s.

3.1.1.2 Spectroelectrochemistry of P1

Spectral changes were explored by UV-Vis- NIR spectrophotometer in a monomer free, 0.1 M TBAPF$_6$, ACN solution in order to search the optical behaviors of **P1** upon doping dedoping processes with potentials between -0.3 V and 1.2 V. Donor-acceptor-donor type polymers usually show two absorption bands and for PDEFPQ (**P1**) these absorption maxima were centered at 447 and 703 nm (Fgure 3.5).

Two simultaneous absorption bands in the red and blue regions of the visible spectrum prove the formation of neutral state green polymers. In the literature, number of these materials are limited and this property increase the importance of **P1**. Actually absorption points are also very important because saturated green color can be acquired when absorptions are around 400 and 700nm. The simultaneous decrease of these peaks upon oxidation yields transmissive oxidized state which is required for the completion of color space and making next generation devices. The second peak at longer wavelength corresponds to the lowest energy π-π* transition of the neutral polymer. The band gap calculated from the onset of this transition was 1.3 eV for **P1**.

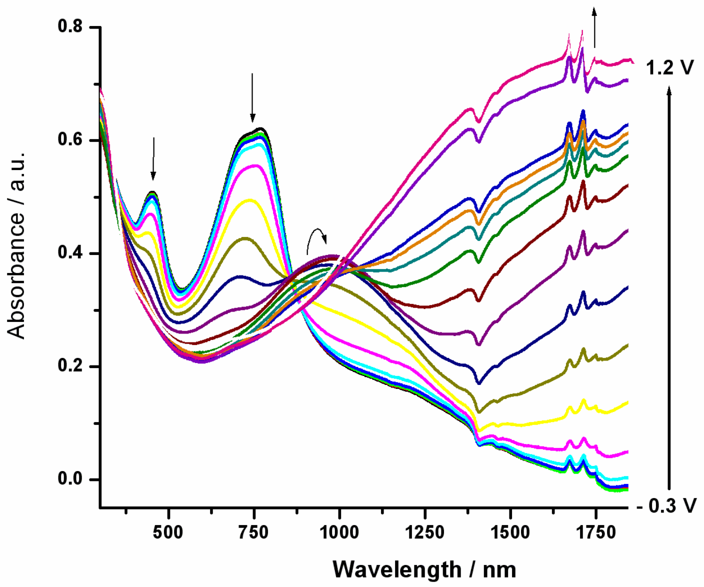

Figure 3. 5 Electronic absorption spectra for PDEFNQ upon p doping between -0.3 V and 1.2 V with 0.1 V potential intervals in a monomer free solution.

In this study ferrocene units were chosen in order to functionalize polymers, and incorporation of ferrocene unit into the polymer backbone makes **P1** a promising multichromic neutral state green to transmissive polymer (Figure 3.6).

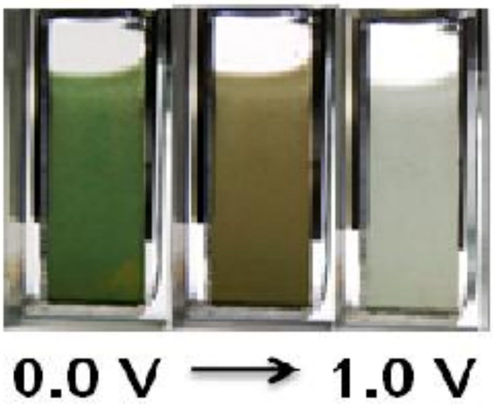

Figure 3. 6 Colors of P1 at its neutral (0.0 V) and different oxidized states.

3.1.1.3 Kinetic Studies of P1

Kinetic studies were conducted in order to determine switching times and percent transmittance changes (ΔT%) of the polymer between neutral and oxidized state.

The polymer films were stepped between two states with 5 s time intervals. As a result of these studies, **P1** revealed 33 % optical contrast with a switching time of 0.8 s. in the visible region and 40 % optical contrast with 1.6 s switching time in the NIR region (Figure 3.7)

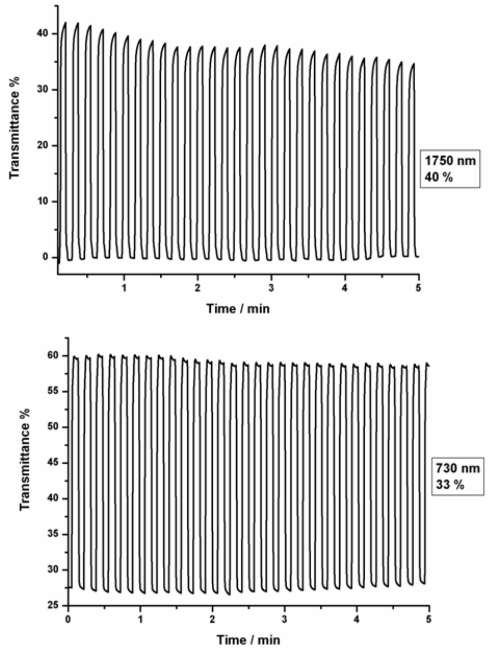

Figure 3. 7 Percent transmittance changes as a function of time at 730 nm and 1750 nm for **P1**.

3.1.2 Electrochemical and Electrochromic Properties of PDEFPQ (P2)

3.1.2.1 Electrochemistry of DEFPQ (M2)

The potentiodynamic electropolymerization of **M2** was performed in 0.1 M $TBAPF_6$/ACN/DCM supporting electrolyte-solvent couple on ITO and the cyclic voltammetry result is shown in Fig 3.8. This figure illustrates the eletroactivity of DEFPQ(**M2**) monomer and formation of corresponding polymer PDEFPQ(**P2**).

Characteristic ferrocene oxidation (Fc / Fc^+) peak was recorded at 0.58 V. The monomer oxidation was achieved at 0.8 V which accompanied with a reversible redox couple resulting from the presence of oligomers and polymer chains. During the first scan, reduction of Fc^+ was blanketed due to the reduction of preliminary chains (Figure 1a)

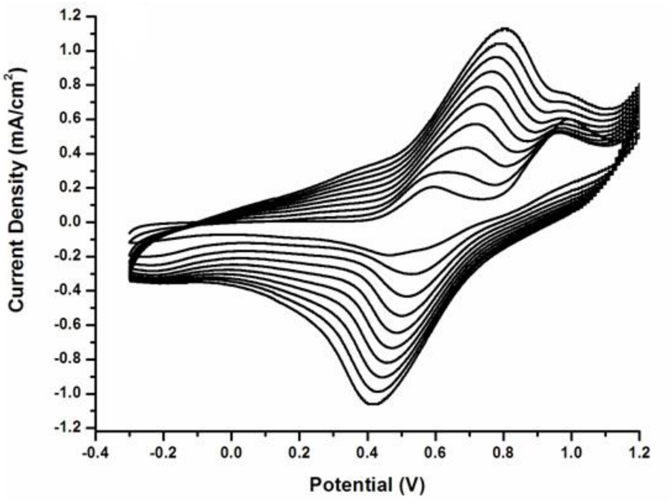

Figure 3. 8 Repeated potential scan electropolymerization of **M2** in 0.1 M TBAPF6/ACN/DCM on ITO electrode.

The polymer also revealed n doping property where a reversible redox couple at-1.95 V and -1.30 V versus the Ag wire pseudo reference electrode, was observed for the n type doping and dedoping processes respectively (Figure 3.9).

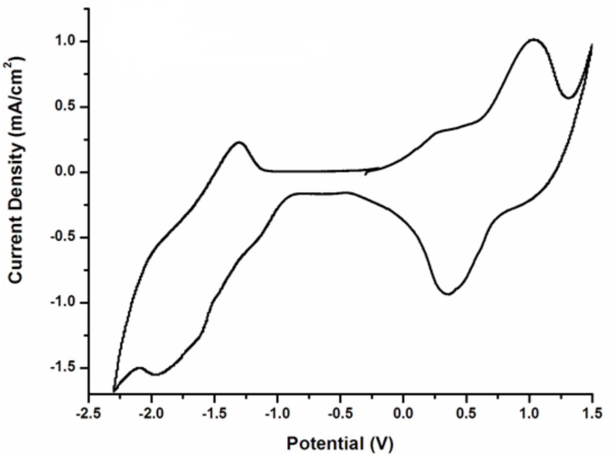

Figure 3. 9 Single scan voltammogram of P2 upon both p and n-type doping

The cyclic voltammograms for both polymer films were recorded at different scan rates (between 100 and 300 mV/s) in monomer free medium and the scan rate dependence of the anodic and cathodic peak currents were observed (Figure 3). This linear dependence illustrates that the charge transfer process for well adhered polymer films were non diffusion controlled (Figure 3.10) [68].

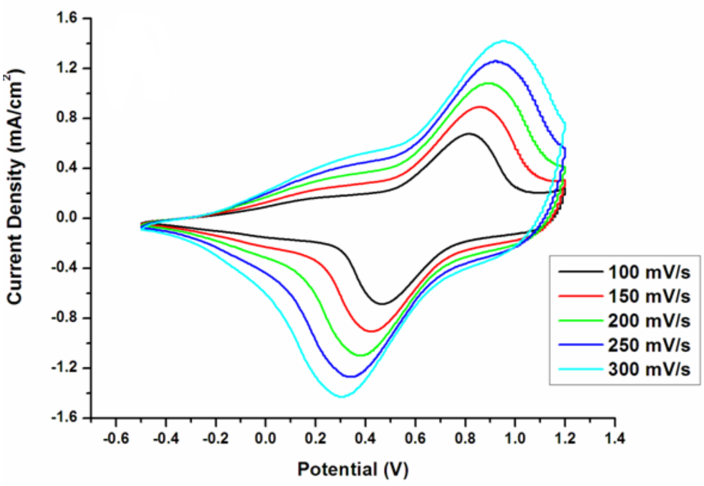

Figure 3. 10 Scan rate dependence of **P2** films at 100, 150, 200, 250, and 300 mV/s.

3.1.2.2 Spectroelectrochemistry of P2

Spectroelectrochemistry studies were performed in the monomer free, 0.1 M $TBAPF_6$, ACN solution to monitor the optical changes upon doping and dedoping processes. UV–Vis-NIR spectra were obtained as a function of applied potential between -0.5 V and 1.0 V. The spectral responses of polymer films to stepwise oxidation were noted as the potential was gradually increased.

As seen in Figure 3.11, **P2** has absorption wavelengths in the visible region which were centered at 447 and 703 nm proving the formation of neutral state green polymer. Optical band gap (E_g) for **P2** was calculated from the onsets of lower energy transition as 1.43 eV which suggests that **P2** can be regarded as a low band gap polymer.

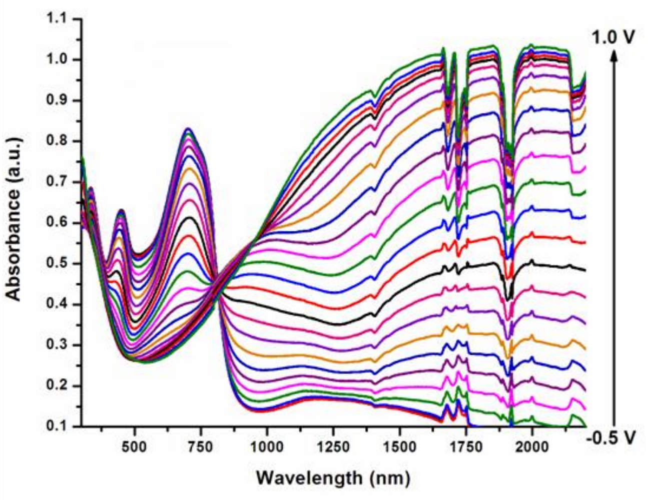

Figure 3. 11 Electronic absorption spectra for PDEFPQ upon p doping between -0.5 V and 1.0 V with 0.1 V potential intervals in a monomer free solution.

Upon stepwise oxidation of polymer film, the absorption in the visible region diminished as the new bands were intensified at around 1000 nm and 1700 nm. These lower energy transitions indicate the formation of charge carriers such as polarons and bipolarons.

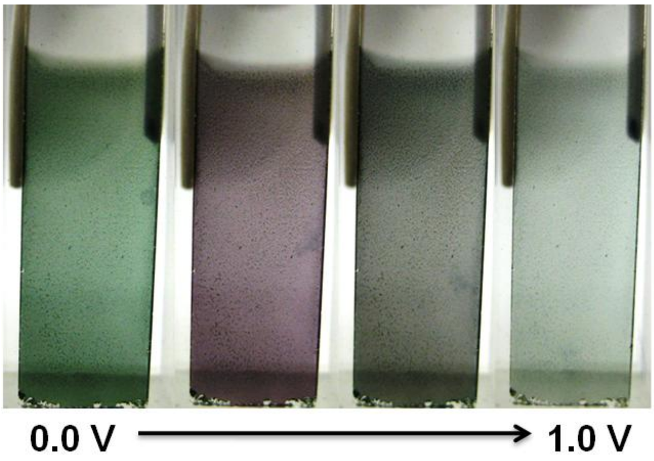

Figure 3. 12 Colors of **P2** at its neutral (0.0 V) and different oxidized states

Figure 3.12 shows the colors of **P2** at its neutral state and different oxidized states. **P2** is also a ferrocene containing quinoxaline derivative polymer like **P1**. Spectroelectrochemical and colorimetric studies showed that incorporation of Fc unit in the polymer backbone resulted in multicolored oxidation states whereas quinoxaline based polymers without ferrocene switched only between green and highly transmissive states.

3.1.2.3 Kinetic Studies of P2

Kinetic studies were conducted in order to determine switching times and percent transmittance changes (ΔT %) of the polymers between their neutral and oxidized states. The polymer films were stepped between the two states with 5 s time intervals. Due to multi-color formation between its two extreme states, ΔT % for **P2** in the visible region was only observable at 703 nm as 40 % with 1.3 s. swiching time. In the NIR region **P2** revealed 22 % optical contrast with a switching time of 1.68 s.

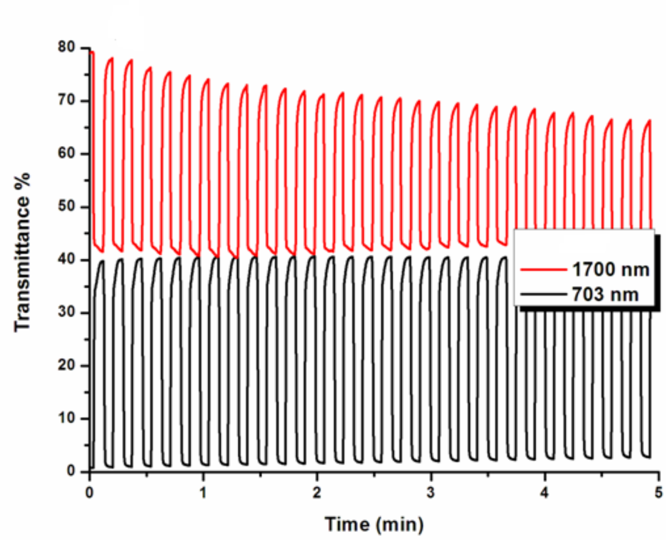

Figure 3. 13 Percent transmittance changes as a function of time at 703 nm and 1700 nm for **P2**.

3.1.3 Electrochemical and Electrochromic Properties of PDEDNQ (P3)

3.1.3.1 Electrochemistry of DEDNQ (M3)

The potentiodynamic electropolymerization for DEDNQ (**M3**) was performed in 0.1 M ($TBAPF_6$) and solvent system was chosen as ACN/DCM (5:95, v: v) mixture. Indium tin oxide coated glass slides (ITO) were used as the working electrode whereto polymer films were produced.

A well-defined reversible redox couple forms an electroactive polymer films. Monomer oxidation potential for **M3** was observed at 0.85 V which was the lowest potential for monomer oxidation among its analogues (Table 3.1).

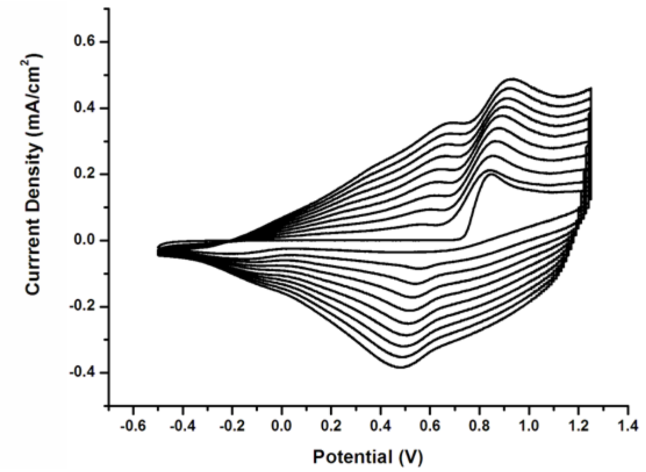

Figure 3. 14 Repeated potential scan electropolymerization of **M2** in 0.1 M TBAPF6/ACN/DCM on ITO electrode.

As mentioned above **P1** and **P2** have both n-doping and p-doping properties. The third derivative **P3** also shows n-doping property with well defined reversible redox couple at -2.05 V/-1.42 V.

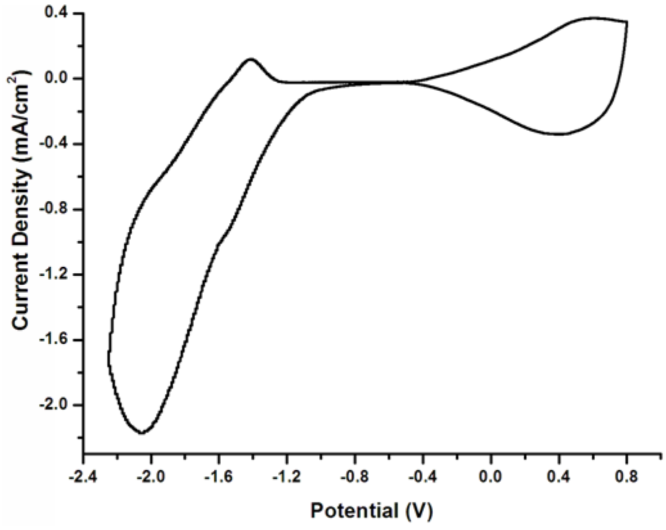

Figure 3. 15 Single scan voltammogram of **P3** upon both p and n-type doping.

The scan rate dependence of the anodic and cathodic peak currents is showed in Figure 3.16 for **P3**. This linear relation proves that the film was well adhered and the electrochemical processes are non-diffusion-controlled [68].

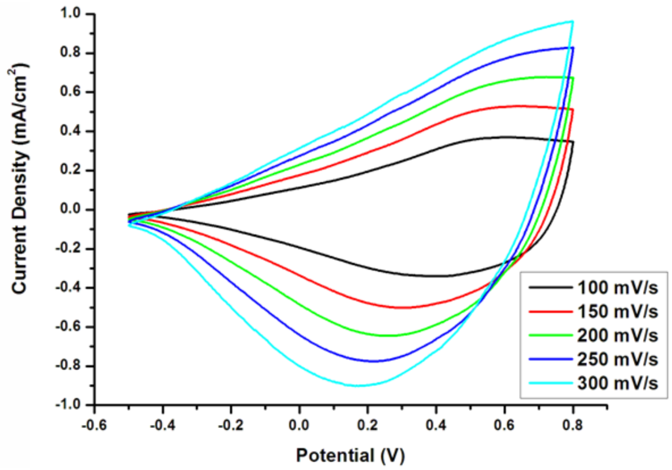

Figure 3. 16 Scan rate dependence of **P3** films at 100, 150, 200, 250, and 300 mV/s.

3.1.3.2 Spectroelectrochemistry of P3

Spectroelectrochemical properties of the polymers were investigated between -0.5 and 1.0 V in 0.1 M $TBAPF_6$/ACN electrolyte-solvent couple and UV-vis-NIR spectra were recorded upon external bias. Figure 3.17 illustrates spectroelectrochemistry of electrochemically prepared **P3** at the reduced state and upon doping.

P3 revealed absorption maxima at 450 and 760 nm which were attributed to low and high energy π-π* transitions. Optical band gap (E_g) for **P3** was calculated from the onset of lower energy transition as 1.24 eV.

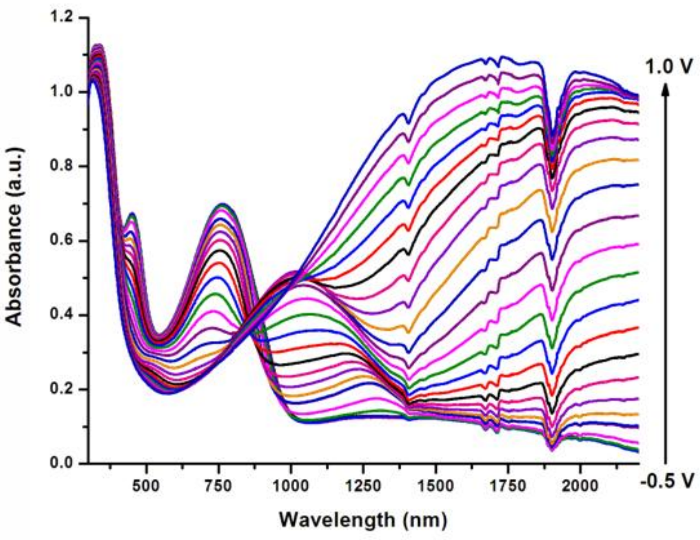

Figure 3. 17 Electronic absorption spectra for PDEDNQ upon p doping between -0.5 V and 1.0 V with 0.1 V potential intervals in a monomer free solution.

Figure 3.17 and Figure 3.18 prove that **P3** is also a neutral state green polymer with a highly transparent oxidized state. When we compare colors of **P3** with its analogus (P**1** and **P2**) derivatives, intermediate color (or colors) between green and transparent can not be observed for **P3**. As a result it can state that incorporation of Fc unit in polymer backbone resulted in multicolored oxidation states.

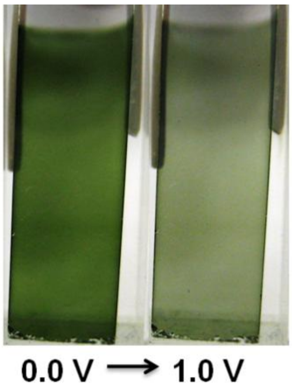

Figure 3. 18 Colors of **P3** at its neutral (0.0 V) and oxidized state.

3.1.3.3 Kinetic Studies of P3

Percent transmittance, switching times and the stabilities of the polymer films upon electrochromic switching between the neutral and oxidized states were recorded in visible and near-IR regions. **P3** film revealed 21 % and 17 % transmittance change between the neutral and oxidized states in the visible region with 0.6 s. and 0.5 s. switching times at the maximum absorption wavelengths (450 nm and 760 nm). In NIR region, **P3** was repetitively switched between its p-type doped/dedoped states and revealed 55 % optical contrast with 0.9 s. switching time.

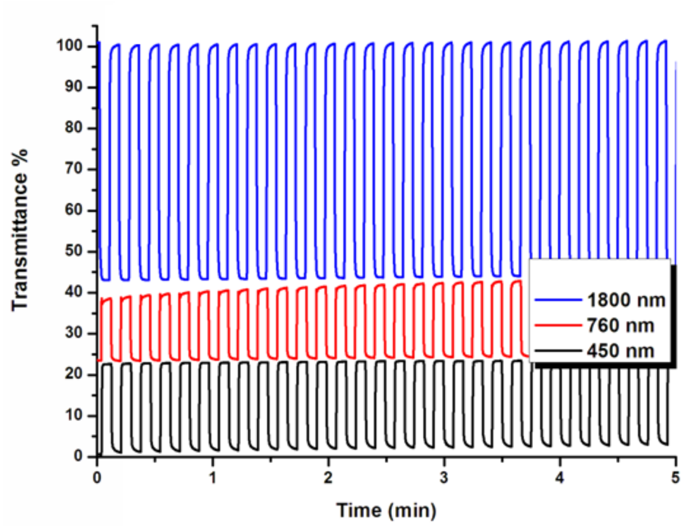

Figure 3. 19 Percent transmittance changes as a function of time at 450 nm, 760 nm and 1800 nm for **P3.**

3.2 Comparison of PDEFNQ (P1), PDEFPQ (P2), PDEDNQ (P3) and PDPEQ

In this study three new monomers were synthesized and electrochemically polymerized, electrochemical and spectroelectrochemical results of related polymers were also explained in the previous parts. In this part, effect of ferrocene unit (electroactive organometallic compound) onto the polymer backbone will be discussed. Figure 3.20 illustrates the structural differences of these four polymers.

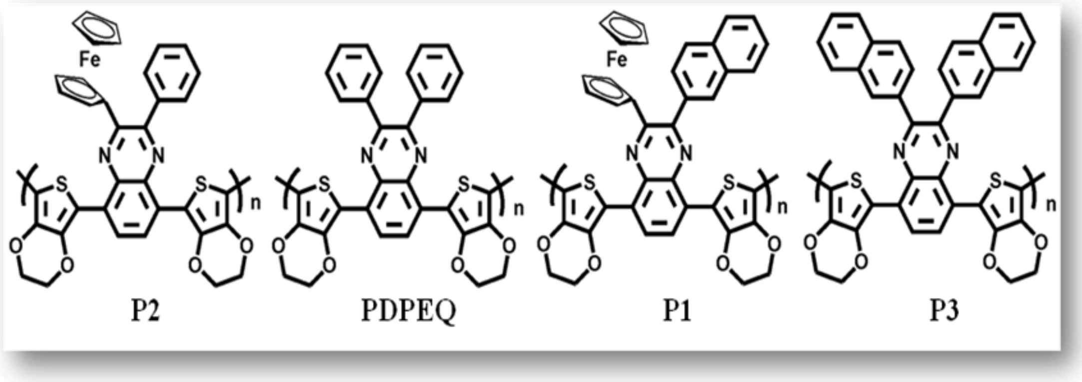

Figure 3. 20 Chemical structures of **P1**, **P2**, **P3**, and **PDPEQ**

Table 1 summarizes electrochemical behaviors of the polymers and their analogues without Fc. As seen, when Fc was replaced by one phenyl unit in **PDPEQ**, both p- and n-type doping/dedoping potentials were increased (**P2**). The trend was also observed for p-type doping/dedoping potentials of **P3** compared to **P1**. This can be attributed to the electroactive behavior of the Fc unit where oxidation of Fc to Fc^+ results in positively charged pendant group on the polymer backbone which makes electron extraction from the polymer more difficult compare to Fc free analogues. Comparison between optical band gaps of all four polymers showed that incorporation of Fc unit as a pendant group increased the band gap of the polymer.

Table 1 Electrochemical and optical results for **P1**, **P2**, **P3**, and **PDPEQ** . [a]Data was taken from ref 69. [b]Fc/Fc$^+$ oxidation potential was observed in the first cycle during CV.

Polymer	**E_{ox}^{mon} (V)**	**$E_{p\text{-doping}}$ (V)**	**$E_{p\text{-dedoping}}$ (V)**	**$E_{n\text{-doping}}$ (V)**	**$E_{n\text{-dedoping}}$ (V)**	**λ_{max} (nm)**	**T%**	**Switchig time (s)**	**E_g^{op} (eV)**
P2	0.58[b] 0.98	1.0	0.35	-1.95	-1.30	447 703 1700	40% 22%	1.3 1.68	1.43
PDPEQ[a]	1.05	0.3	-0.02	-1.55	-1.10	448 732 1800	35% 29% 77%	1.2 0.7 2	1.01
P1	0.72[b] 1.1	0.85	0.42	-1.70	-1.35	450 760 1750	33% 40%	0.8 1.6	1.3
P3	0.85	0.60	0.35	-2.05	-1.42	450 760 1800	21% 17% 57%	0.6 0.5 0.9	1.24

Spectroelectrochemical and colorimetric studies showed that incorporation of Fc unit in polymer backbone resulted in multicolored oxidation states whereas quinoxaline based polymers without ferrocene switched only between green and highly transmissive states (Figure 3.6, Figure 3.12, Figure 3.18). Intermediate colored states appeared due to contribution of orange and blue colors which are the characteristic colors of Fc and Fc$^+$ respectively. This was also proven by the different spectral response of Fc containing polymers upon stepwise oxidation compared to that of non-containing ones (Figure 3.5, Figure 3.11, Figure 3.17).

CHAPTER 4

CONCLUSION

The donor-accetor-donor type three new monomers were synthesized by Stille coupling reactions and NMR was used for the characterization of these materials. Electrochemical polymerization method was used for polymerization of corresponding monomers. As a result of cyclic voltammetry, spectroelectrochemistry, kinetic studies and switching experiments electrochemical properties these conducting polymers were investigated.

All the three materials are quinoxaline and EDOT based conducting polymers. PDEFNQ (**P1**) is a ferrocene functionalized, both p and n dopable donor-acceptor-donor type conjugated polymer. **P1** is a neutrally green polymer but it has multicolored states with a transmissive oxidized state.

Structural design for PDEFPQ (**P2**) and PDEDNQ (**P3**) were accomplished in order to have a better comparison and understanding on the pendant group effect on electrochromic properties of these green to transmissive conjugated polymers. Summary of results showed that incorporation of Fc substituent enhanced the optical contrast in the visible region which in turn resulted in better transparency for the oxidized state (comparison is made between **P2** and PDPEQ or between **P1** and **P3**). Only phenyl pendant group as in PDPEQ resulted in higher optical contrast with a longer switching time than that of naphtyl substituted **P3**. However, Fc pendant group bearing polymers (**P1** and **P2**) revealed multicolored electrochromism which is an effect of independent electrochromic switching of Fc. Thus, multicolored states with green to transmissive switching polymers could be achieved by Fc substitution.

REFERENCES

[1] M.S. Freund, B. Deore, *Self-Doped Conducting Polymers*, **2007**, England, p1.

[2] G. Inzelt, *Conducting Polymers (A New Era in Electrochemistry)*, **2008**, Berlin Heidelberg, p1.

[3] C. K. Chiang, Y. W. Park, A. J. Heeger, H. Shirakawa, E. J. Louis, A. G. MacDiarmid, *Phys. Rev. Lett.*, **1977**, 39, 1098.

[4] a) A. F. Diaz, *Chem. Scr.*, **1981**, 17,142. b)G. Tourillon, F. J. Garnier, *J. Electroanal. Chem.*, **1982**, 135,173. c) A. F. Diaz, K. K. Kanazawa, G. P. Gardini, *J. Chem. Soc., Chem. Commun*., **1979**, 635. d) G. Grem, G. Leditzky, B. Ullrich, G. Leising, *Adv. Mater.*, **1992**, 4, 36. e) J. H. Burroughes, D. D. C. Bradley, A. R. Brown, R. N. Marks, K. MacKay, R. H. Friend, P. L. Burn, A. B. Holmes, *Nature*, **1990**, 347, 539. f) J. Rault-Berthelot, J. Simonet, *J. Electrochem. Soc.*, **1985**, 182, 187. g) A. G. MacDiarmid, A. J. Epstein, *Faraday Discuss. Chem. Soc.*, **1989**, 88, 317.

[5] M. E. G. Lyons, *Electroactive Polymer Electrochemistry*, **1994**, New York, p48.

[6] K. Shimamura, F. E. Karasz, J. A. Hirsch, J. C. Chien, *Makromol. Chem. Rapid Commun.*, **1981**, 2, 443.

[7] J. L. Bredas, G. B. Street, *Acc. Chem. Res.*, **1985**, 18, 309.

[8] C. Pratt, *Conducting Polymers*.

[9] K. Fesser, A. R. Bishop, D. K. Campbell, *Phys. Rev. B*, **1983**, 27, 4804.

[10] D. L. Wise, G. E. Wnek, D. J. Trantolo, T. M. Cooper, J. D. Gressser, *Electrical And Optical Polymer Systems*, **1998**, New York, pp 49-52.

[11] A. J. Heeger, *J. Phys. Chem. B*, **2001**, 105, 8475.

[12] A. D. Child, J. R. Reynolds, *J. Chem. Soc., Chem. Commun*, **1991**, 1779.

[13] S. Alkan, L. Toppare, Y. Hepuszer, Y. Yağcı, *J. Polym. Sci. Part A: Polym. Chem.*, **1999**, 37, 4218.

[14] D. M. de Leeuw, M. M. J. Simenon, A. R. Brown, R. E. F. Einerhand, *Synth. Met.*, **1997**, 87, 53.

[15] C. J. DuBois, F. Larmat, D. J. Irvin, J. R. Reynolds, *Synth. Met.*, **2001**, 119, 321.

[16] C. J. DuBois, K. A. Abboud, J. R. Reynolds, *J. Phys. Chem. B*, **2004**, 108, 8550.

[17] C. J. DuBois, J. R. Reynolds, *Adv. Mater.*, **2002**, 14, 1844.

[18] D. Kumar, R. C. Sharma, *Eur. Polym. J.*, **1998**, 34, 1053.

[19] G. A. Sotzig, PhD Thesis, University of Florida, (**1997**).

[20] P.M. Beaujuge, S. Ellinger, J.R. Reynolds, *Adv. Mater.*, **2008,** 20, 2772.

[21] a) S. Ryu, I. Yoo, S. Song, B. Yoon, J. M. Kim, *J. Am. Chem. Soc.*, **2009**, 131, 3800.

b) Y. Long, H Chen, Y. Yang, H. Wang, Y. Yang, N. Li, K. Li, J. Pei, F. Liu, *Macromolecules*, **2009**, 42, 6501.

c) R. C. Smith, A. G. Tennyson, M. H. Lim, S. J. Lippard, *Org. Lett.,* **2005**, 7, 3573.

d) D. T. McQuade, A. E. Pullen, T. M. Swager, *Chem. Rev.*, **2000**, 100, 2537.

[22] a) N. R. Evans, L. S. Devi, C. S. K. Mak, S. E. Watkins, S. I. Pascu, A. Kohler, R. H. Friend, C. K. Williams, A. B. Holmes., *J. Am. Chem Soc.*, **2006**, 128, 6647. b) Q. Huang, G. A. Evmenenko, P. Dutta, P. Lee, N. R. Armstrong, T. J. Marks, *J. Am. Chem. Soc.*, **2005,** 127, 10227. c) M. H. Song, D. Kabra, B. Wenger, R. H. Friend, H. J. Snaith., *Adv. Funct. Mater.*, **2009**, 19, 2130. d) P. Zacharias, M. C. Gather, A. Köhnen, N. Rehmann, K. Meerholz, *Angew. Chem. Int. Ed.*, **2009**, 48, 4038.

[23] a) Y. He, G. Zhao, J. Min, M. Zhang, Y. Li, *Polymer*, **2009**, 50, 5055. b) J. C. Bijleveld, A. P. Zoombelt, S. G. J. Mathijssen, M. M. Wienk, M. Turbiez, D. M. Leeuw, R. A. J. Janssen, *J. Am. Chem. Soc.*, **2009**, 13, 16616. c) C. J. Brabec, N. S. Sariciftci, J. C. Hummelen., *Adv. Funct. Mater.*, **2001**, 11, 15. d) N. S. Sariciftci, D. Braun, C. Zhang, V. Srdanov, A. J. Heeger, F. Stucky, F. Wudl, *App. Phys. Lett.*, **1993**, 62, 585. e) M. Horie, I. W. Shen, S. M. Tuladhar, H. Leventis, S. A. Haque, J. Nelson, B. R. Saunders, M. L. Turner, *Polymer*, **2010**, 51, 1541.

[24] a) D. S. H. Charrier, T. Vries, S. G. J. Mathijssen, E. J. Geluk, E. C. P. Smits, M. Kemerink, R. A. J. Janssen, *Org. Electron.*, **2009**, 10, 994. b) H. H. Fong, V. A. Pozdin, A. Amassian, G. G. Malliaras, D. M. Smilgies, M. He, S. Gasper, F. Zhang, M. Sorensen, *J. Am. Chem. Soc.*, **2008**, 130, 13202. c) P. M. Beaujuge, W. Pisula, H. N. Tsao, S. Ellinger, K. Mullen, J. R. Reynolds., *J. Am. Chem. Soc.*, **2009**, 131, 7514. d) I. McCulloch, M. Heeney, C. Bailey, K. Genevicius, I. MacDonald, M. Shkunov, D. Sparrowe, S. Tierney, R. Wagner, W. Zhang, M. L. Chabinyc, R. J. Kline, M. D.

McGehee, M. F. Toney., *Nat. Mater.*, **2006**, 5, 328. e) L. L. Chua, J. Zaumseil, J. F. Chang, E. C. W. Ou, P. K. H. Ho, H. Sirringhaus, R. H. Friend, *Nature*, **2005**, 434, 194. f) N. Stutzmann, R. H. Friend, H. Sirringhaus, *Science*, **2003**, 299, 1881.

[25] a) S. Celebi, D. Baran, A. Balan, L. Toppare, *Electrochimi. Acta*, **2010**, 55, 2373. b) G. Sonmez, H. B. Sonmez, C. K. F. Shen, R. W. Jost, Y. Rubin, F. Wudl, *Macromolecules*, **2005**, 38, 669. c) I Schwendeman, R Hickman, G Sonmez, P Schottland, K Zong, DM Welsh, JR. Reynolds, *Chem. Mater*, **2002**, 14, 3118. d) A. Balan, G. Gunbas, A. Durmus, L. Toppare, *Chem. Mater.*, **2008**, 20, 7510. e) A. Kumar, S. Jang, J. Padilla, T. F. Otero, G. A. Sotzing, *Polymer*, **2008**, 49, 3686.

[26] R. J. Mortimer, *Chem. Soc. Rev.*, **1997**, 26, 147.

[27] D. R. Rosseinsky, R. J. Mortimer, *Adv. Mater.*, **2001**, 13, 783.

[28] A. A. Argun, P. H. Aubert, B. C. Thompson, I. Schwendeman, C. L. Gaupp, J. Hwang, N. J. Pinto, D. B. Tanner, A. G. MacDiarmid, J. R. Reynolds, *Chem. Mater.*, **2004**, 16, 4401.

[29] M. A. Habib, *Electrochem. Transition*, **1992**, 51.

[30] R. J. Mortimer, *Electrochim. Acta*, **1999**, 44, 2971.

[31] P. R. Somani, S. Radhakrishnan, *Mater. Chem. Phys.*, **2003**, 77, 117.

[32] A. Kumar, D. M. Welsh, M. C. Morvant, F. Piroux, K. A. Abboud, J. R. Reynolds, *Chem. Mater.*, **1998**, 10, 896.

[33] S. A. Sapp, G. A. Sotzing, J. R. Reynolds, *Chem. Mater.*, **1998**, 10, 2101.

[34] G. Sonmez, H. B. Sonmez, C. K. F. Shen, R. W. Jost, Y. Rubin, F. Wudl, *Macromolecules*, **2005**, 38, 669.

[35] I. Schwendeman, R. Hickman, G. Sonmez, P. Schottland, K. Zong, D. Welsh, J. R. Reynolds, *Chem. Mater.*, **2002**, 14, 3118.

[36] K. Fesser, A. R. Bishop, D. K. Campbell, *Phys. Rev. B*, **1983**, 27, 4804.

[37] J. Roncali, *Chem. Rev.*, **1997**, 97, 173.

[38] D. M. Welsh, A. Kumar, E. W. Meijer, J. R. Reynolds, *Adv. Mater.*, **1999**, 11, 1379.

[39] A. Balan, Ms Thesis, Middle East Technical University, (**2009**)

[40] C. A. Thomas, K. Zong, K. A. Abboud, P. J. Steel, J. R. Reynolds, *J. Am. Chem. Soc.*, **2004**, 126, 16440.

[41] G. Gunbas, Ms Thesis, Middle East Technical University, (**2007**)

[42] G. Sonmez, *Chem. Commun.*, **2005**, 5251.

[43] G. Sonmez, C. K. F. Shen, Y. Rubin, F. Wudl, *Angew. Chem. Int. Ed.*, **2004**, 43, 1498.

[44] A. Durmus, G. E. Gunbas, P. Camurlu, L. Toppare, *Chem Commun.*, **2007**, 3246.

[45] A. Durmus, G. E. Gunbas, L. Toppare, *Chem. Mater.*, **2007**, 19, 6247.

[46] G. E. Gunbas, A. Durmus, L. Toppare, *Adv. Mater*, **2008**, 20, 691.

[47] G. E. Gunbas, A. Durmus, L. Toppare, *Adv. Funct. Mater.*, **2008**, 18, 2026.

[48] P. M. Beaujuge, S. Ellinger J. R. Reynolds, *Adv. Mater.*, **2008**, 20, 2772.

[49] a) A. Togni, T. Hayashi , *Ferrocene-Homogeneous Catalysis, Organic Synthesis and Material Science,* **1995**, VCH, New York. b) G. Wilkinson, *J. Organomet. Chem.,* **1975**, *100*, 273.

[50] R. D. A. Hudson, *Journal of Organometallic Chemistry*, **2001**, 47, 637.

[51] M. O. Wolf, *Adv. Mater.*, **2001**, 13, 545.

[52] S. Takahashi, M. Kariya, T. Yatake, K. Sonogashira, N. Hagihara, *Macromolecules*, **1978**, 11, 1063.

[53] H. B. Fyfe, M. Miekuz, D. Zargarian, N. J. Taylor, T. B. Marder, *J. Chem. Soc., Chem. Commun.*, **1991**, 188.

[54] M. J. Irwin, J. J. Vittal, R. J. Puddephatt, *Organometallics*, **1997**, 16, 3541.

[55] S. J. Davies, B. F. G. Johnson, J. Lewis, P. R. Raithby, *J. Organomet. Chem.*, **1991**, 414, C51.

[56] A. Ion, I. Ion, A. Popescu, M. Ungureanu, J. C. Moutet, E. Saint-Aman, *Adv. Mater.*, **1997**, 9, 711.

[57] J. Chen, C. O. Too, G. G. Wallace, G. F. Swiegers, B.W. Skelton, A. H. White, *Electrochim. Acta*, **2002**, 47, 4227.

[58] S. Ifuku, Y. Tsujii, H. Kamitakahara, T. Takano, F. Nakatsubo, *J. Polym. Sci., Part A: Polym. Chem.*, **2005**, 43, 5023.

[59] M. E. Plonska, A. Bettencourt-Dias, A. L. Balch, K. Winkler, *Chem. Mater.*, **2003**, 15, 4122.

[60] J. Xu, Y. Tian, R. Peng, Y. Xian, Q. Ran, L. Jin, *Electrochem. Commun.*, **2009**, 11, 1972.

[61] Y. Zhu, M. O. Wolf, *Chem. Mater.*, **1999**, 11, 2995.

[62] L. E. Harrington, J. F. Britten, M. J. McGlinchey, *Can. J. Chem.*, **2003**, 81, 1180.

[63] B. A. Da Silveria Neto, A. L. Sant′Ana, G. Ebeling, S. R. Goncalves, E. V. U. Costa, H. F. Quina, J. Dupont, *Tetrahedron*, **2005**, 61, 10975.

[64] Y. Tsubata, T. Suzuki, T. Miyashi, Y. Yamashita, *J. Org. Chem.*, **1992**, 57, 6749.

[65] S. S. Zhu, T. M. Swager, *J. Am. Chem. Soc.*, **1997**, 119, 12568.

[66] a) M. A. Khan,W. Xu, K. Haq, Y. Bai, F.Wei, X. Y. Jiang, Z. L. Zhang, W. Q. Zhu, *J. Phys. D: Appl. Phys.*, **2007**, 40, 6535. b) E. J. Meijer, D. M. de Leeuw, S. Setayesh, E. van Veenendaal, B. H. Huisman, P. W. M. Blom, J. C. Hummelen, U. Scherf , T. M. Klapwijk, *Nature Materials*, **2003**, 2, 678.

[67] C. J. DuBois, J. R. Reynolds, *Adv. Mater.*, **2002**, 14, 1844.

[68] G. Sonmez, I. Schwendeman, P. Schottland, K. Zong, J. R. Reynolds, *Macromolecules*, **2003**, 36, 639.

[69] G. Gunbas, A. Durmus, L. Toppare, *Adv. Mater.*, **2008**, 20, 691.

APPENDIX A

NMR DATA

NMR spectra were recorded on a Bruker DPX 400.

Chemical shifts δ are reported in ppm relative to $CHCl_3$ (^1H: δ=7.27), $CDCl_3$ (^{13}C: δ=77.0) and CCl4 (^{13}C: δ=96.4) as internal standards.
^1H and ^{13}C NMR spectra of products are given below.

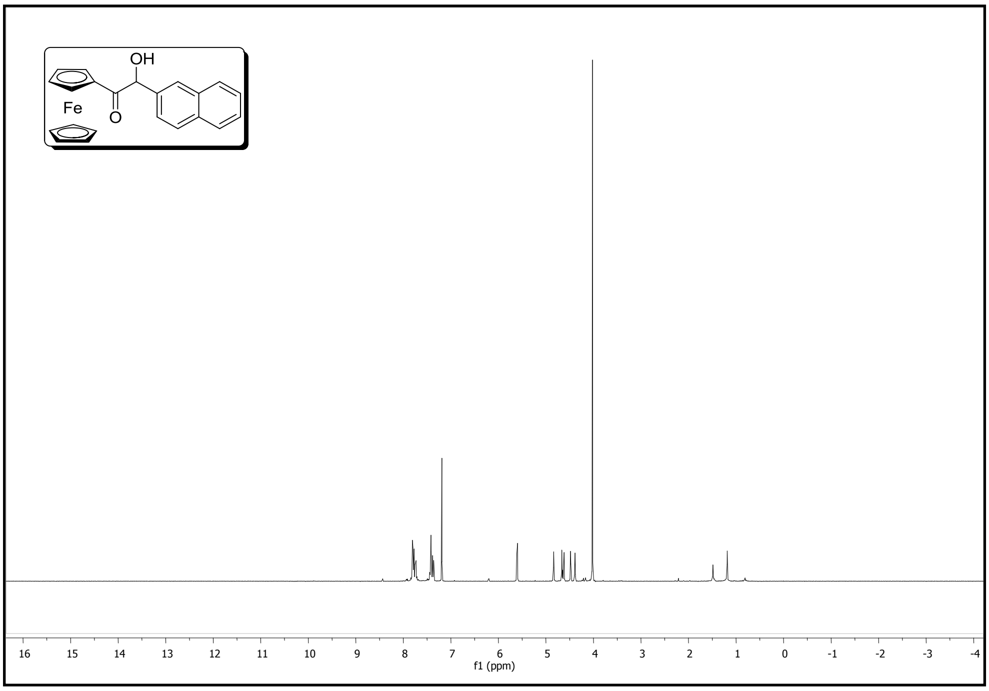

Figure A. 1 ^1H-NMR spectrum of 2-Hydroxy-2-(naphthalen-2-yl)-1-ferrocenylethanone **(3)**

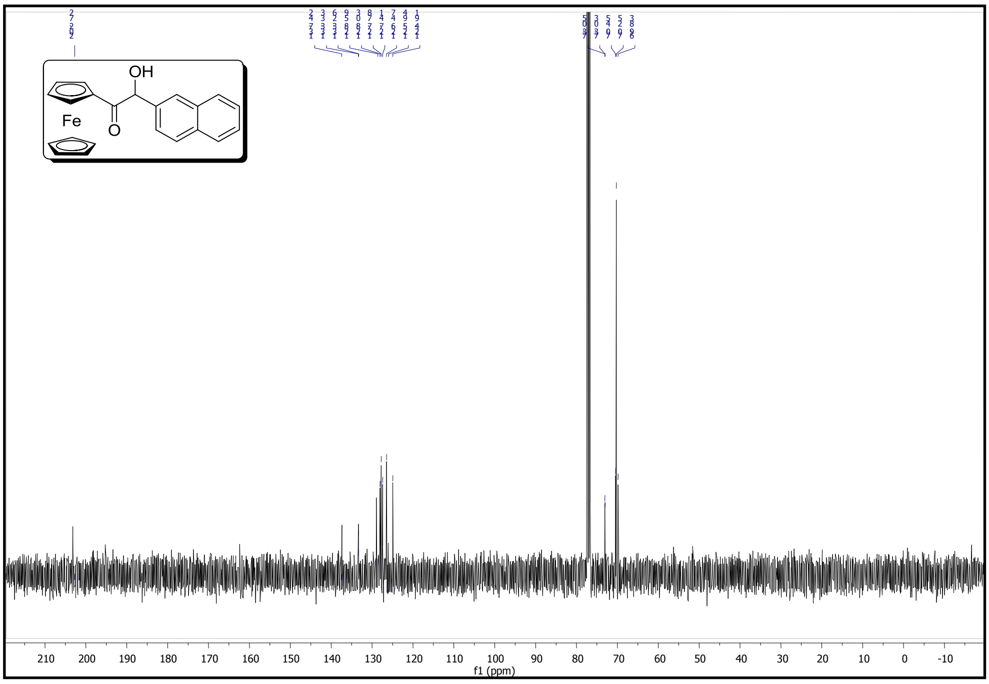

Figure A. 2 ^{13}C-NMR spectrum of 2-Hydroxy-2-(naphthalen-2-yl)-1-ferrocenylethanone **(3)**

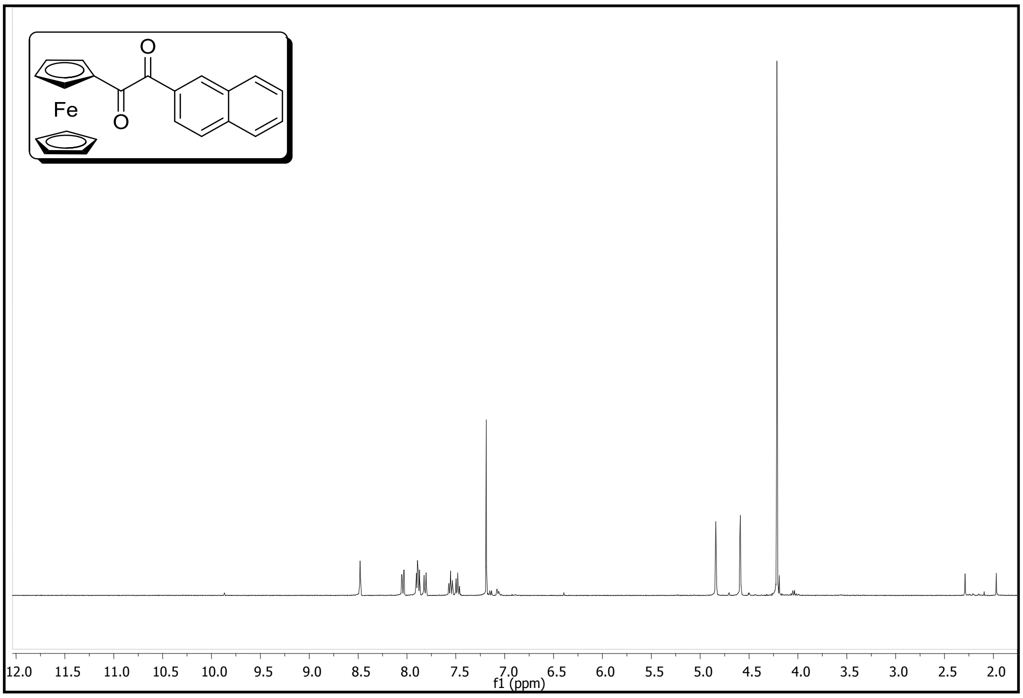

Figure A. 3 ^{1}H-NMR spectrum of 1-ferrocenyl-2-naphthylethanedione **(4)**

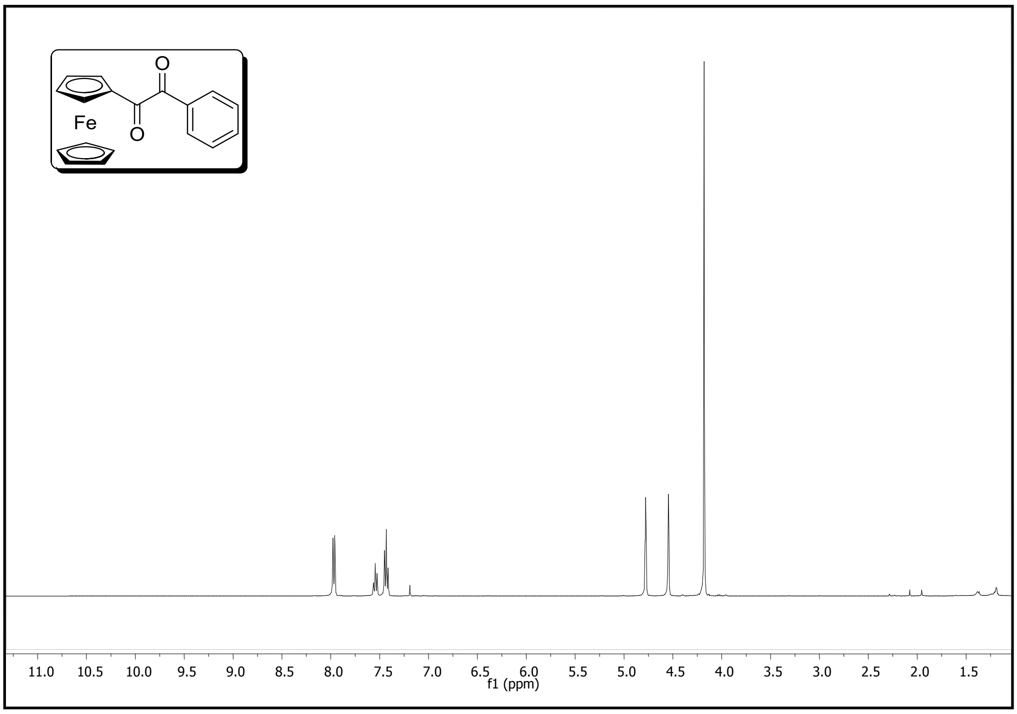

Figure A. 4 ^{1}H-NMR spectrum of 1-ferrocenyl-2-phenylethanedione **(7)**

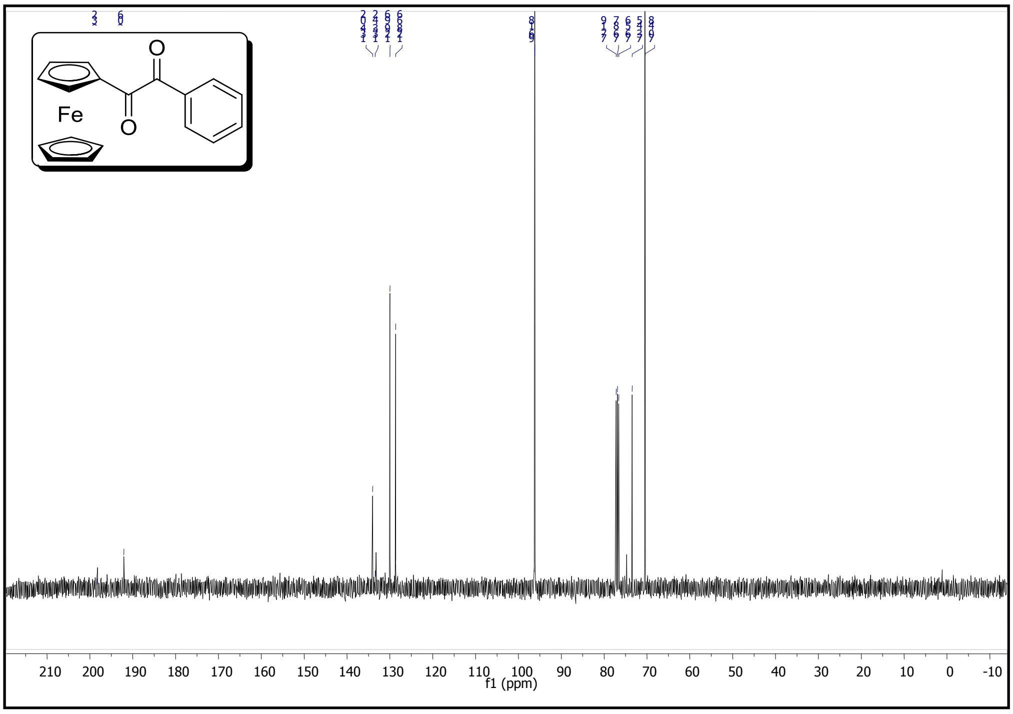

Figure A. 5 ^{13}C-NMR spectrum of 1-ferrocenyl-2-phenylethanedione **(7)**

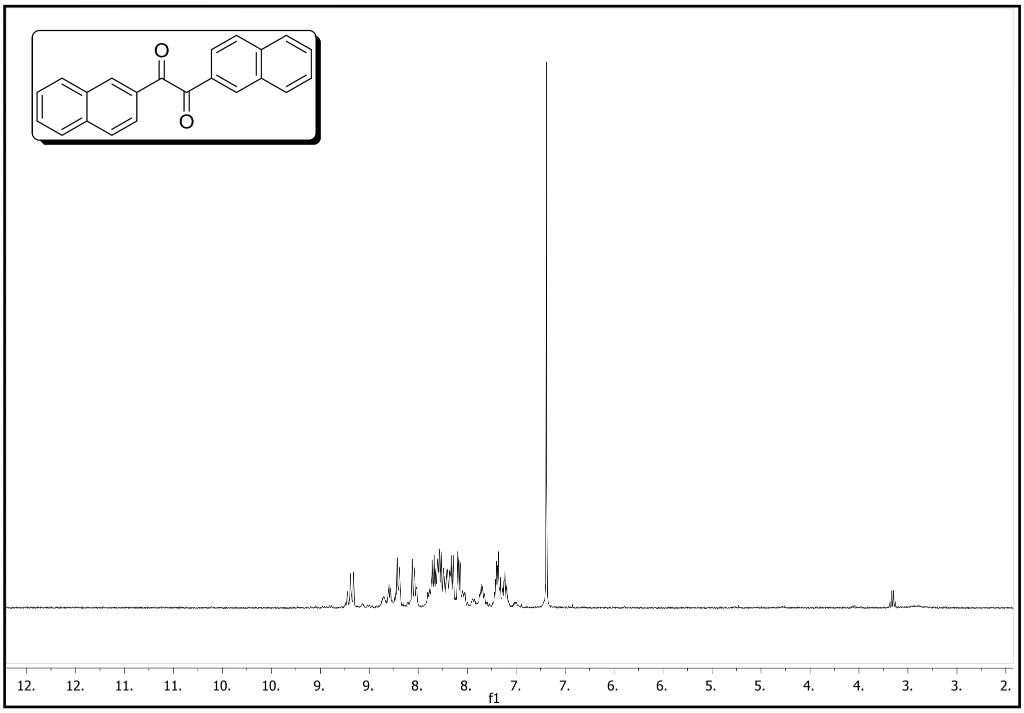

Figure A. 6 ^{1}H-NMR spectrum of 1,2-di(naphthalen-2-yl)ethane-1,2-dione **(9)**

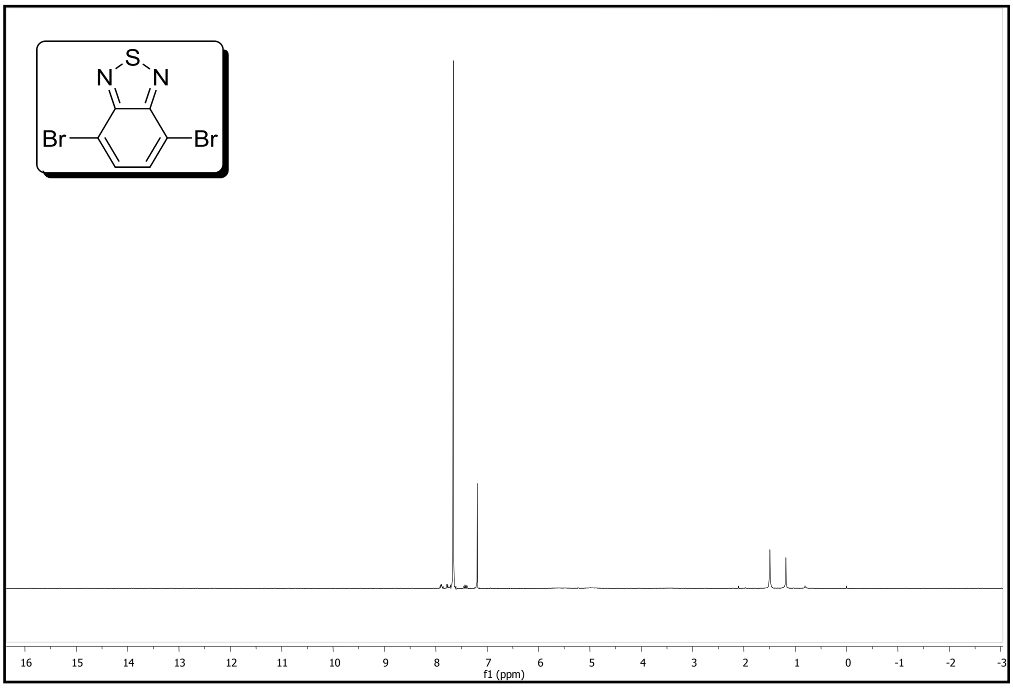

Figure A. 7 ^{1}H-NMR spectrum of 4, 7-Dibromo-2.1.3-benzothiadiazole **(11)**

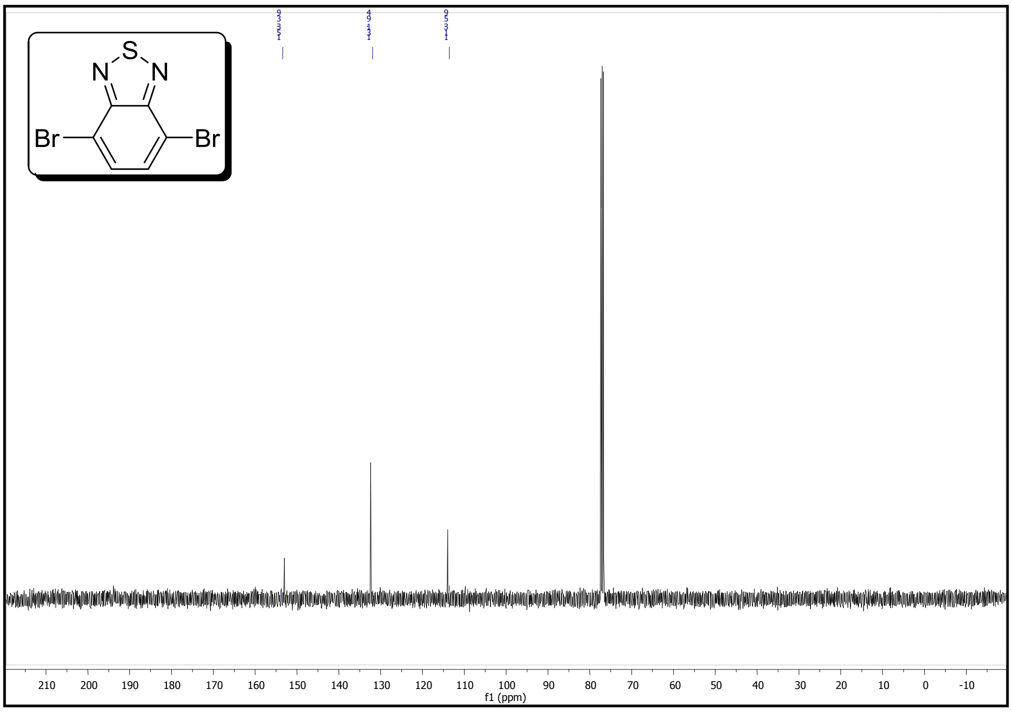

Figure A. 8 ^{13}C-NMR spectrum of 4, 7-Dibromo-2.1.3-benzothiadiazole **(11)**

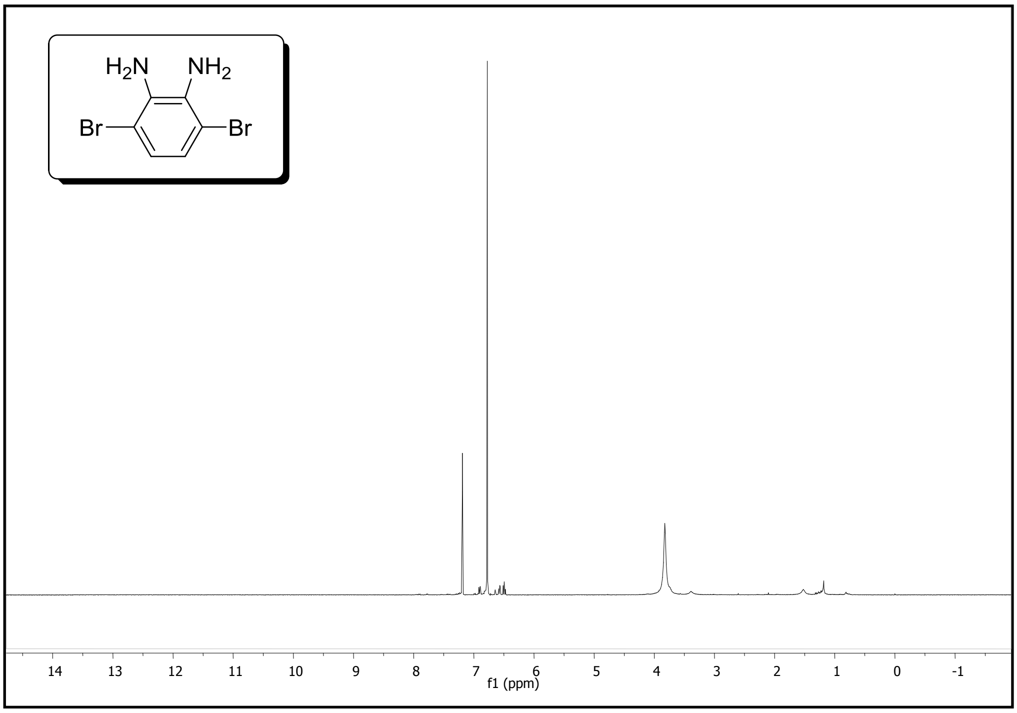

Figure A. 9 ^{1}H-NMR spectrum of 3,6-dibromo-1,2-phenylenediamine **(12)**

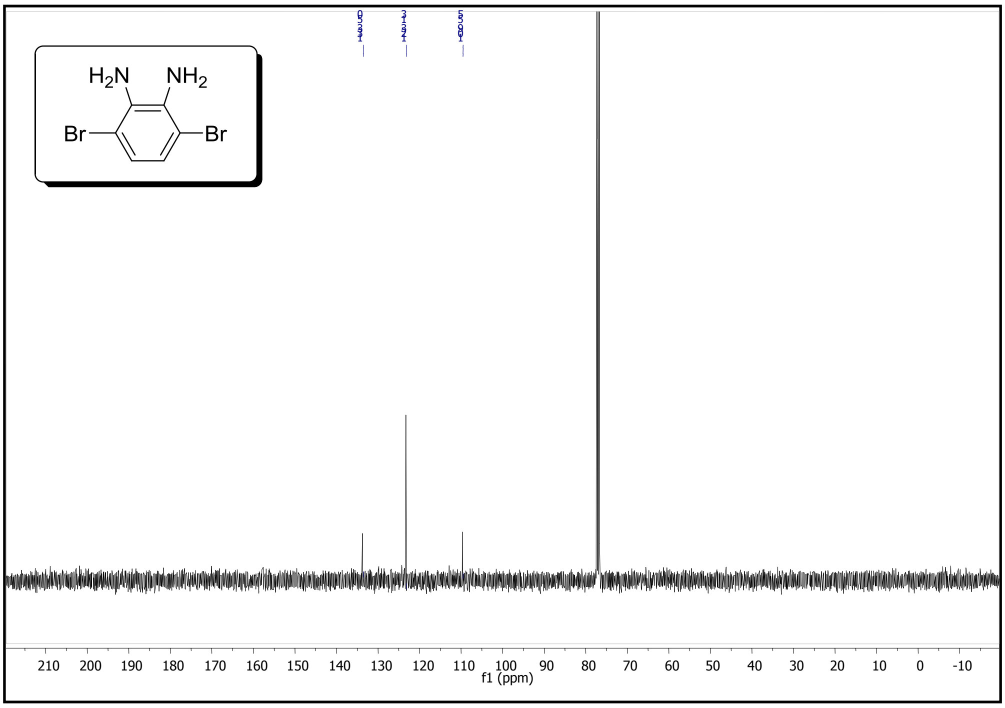

Figure A. 10 ^{13}C-NMR spectrum of 3, 6-dibromo-1, 2-phenylenediamine **(12)**

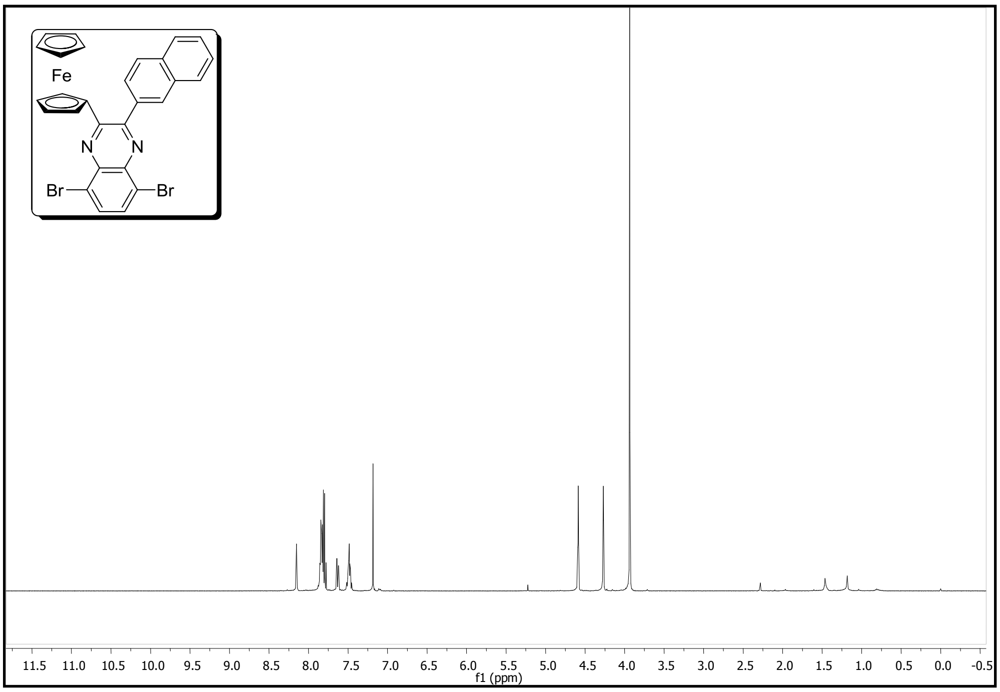

Figure A. 11 ^{1}H-NMR spectrum of 5, 8-dibromo-2-(naphthalen-2-yl)-3-ferrocenyl-4a, 8a-dihydroquinoxaline **(15)**

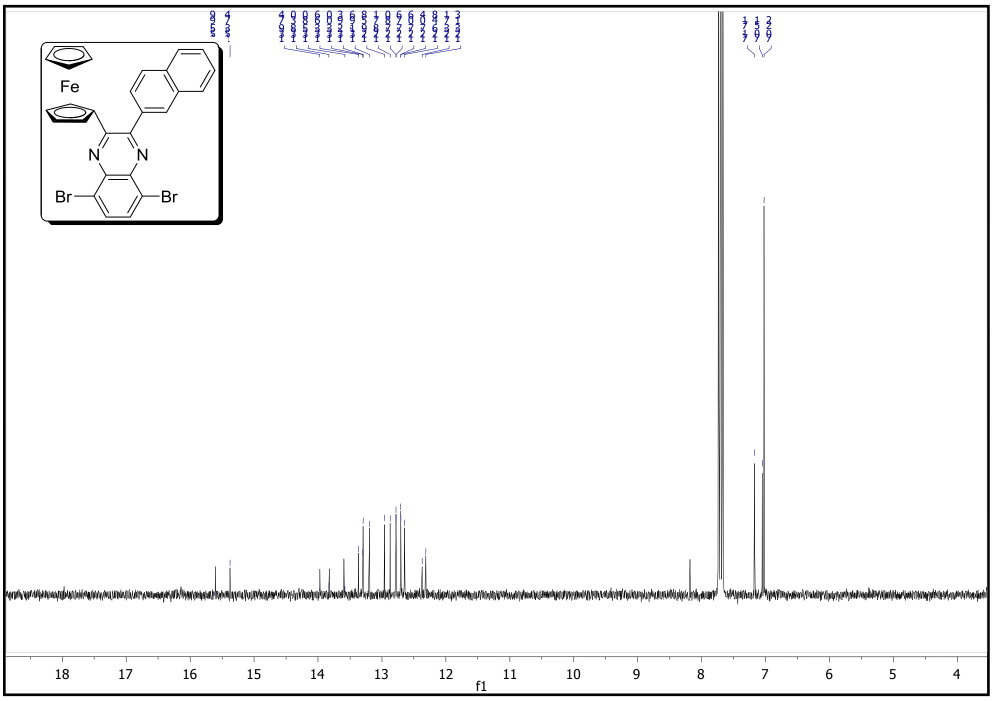

Figure A. 12 ^{13}C-NMR spectrum of 5,8-dibromo-2-(naphthalen-2-yl)-3-ferrocenyl-4a,8a-dihydroquinoxaline **(15)**

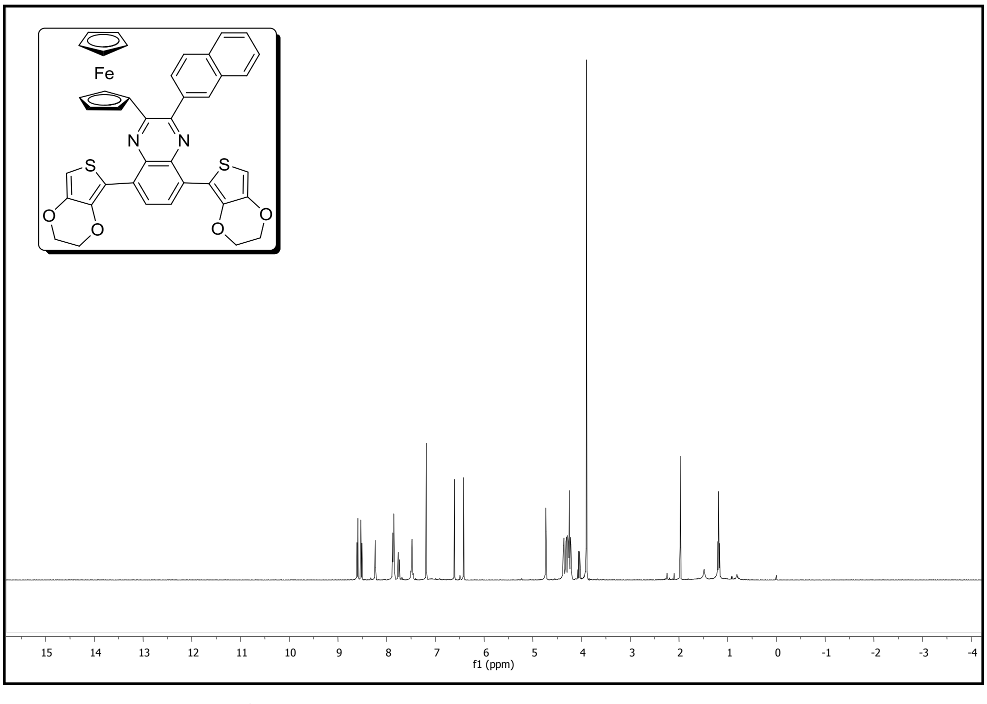

Figure A. 13 ^{1}H-NMR spectrum of 5,8-bis(2,3-dihydrothieno[3,4-b][1,4]dioxin-5-yl)-2-(naphthalen-2-yl)-3-ferrocenyl-4a,8a-dihydroquinoxaline (**M1)**

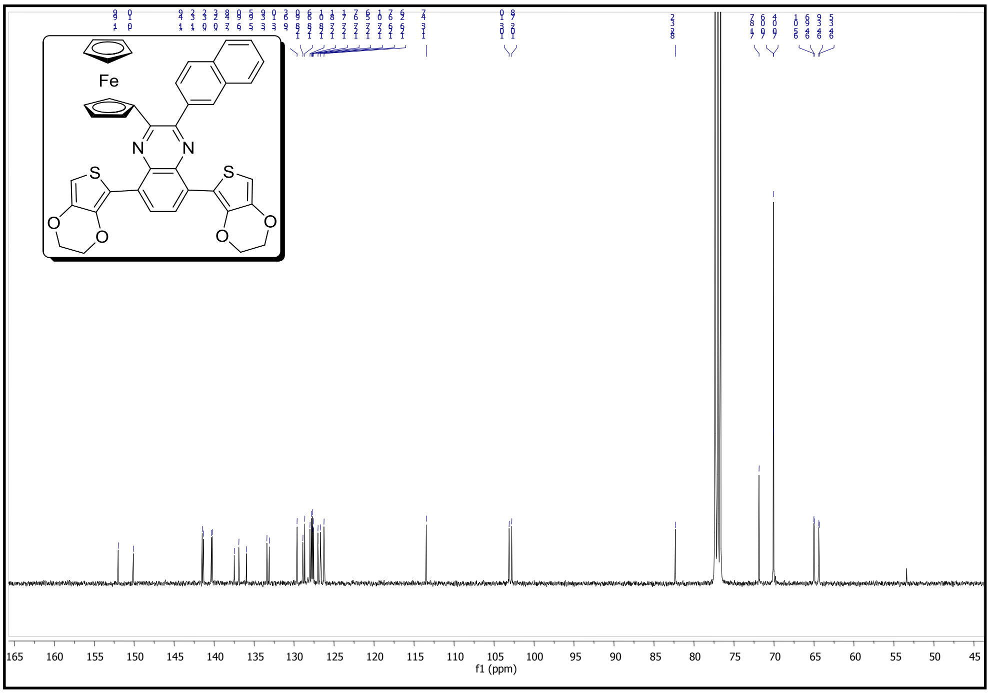

Figure A. 14 ^{13}C-NMR spectrum of 5,8-bis(2,3-dihydrothieno[3,4-b][1,4]dioxin-5-yl)-2-(naphthalen-2-yl)-3-ferrocenyl-4a,8a dihydroquinoxaline (**M1)**

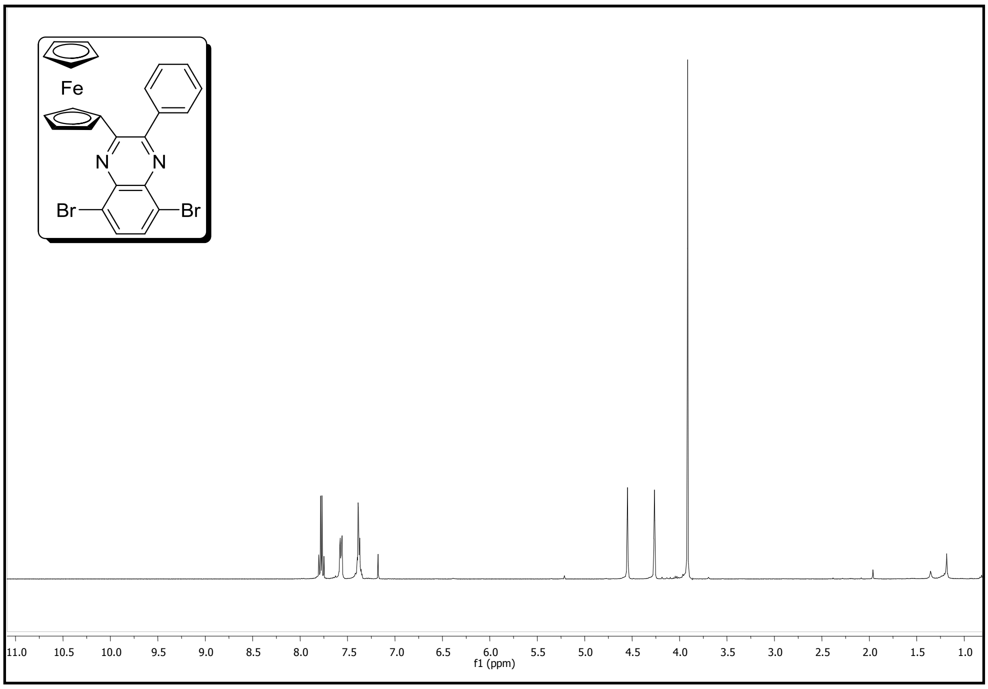

Figure A. 15 ^{1}H-NMR spectrum of 5,8-dibromo-2-phenyl-3-ferrocenylquinoxaline **(16)**

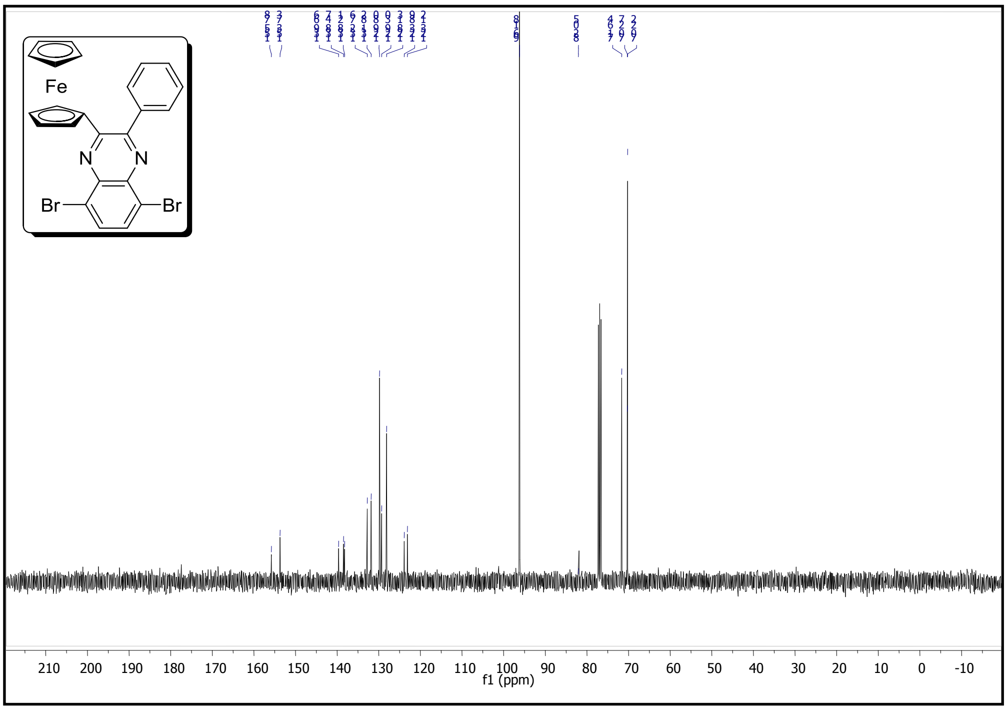

Figure A. 16 ^{13}C-NMR spectrum of 5,8-dibromo-2-phenyl-3 ferrocenylquinoxaline (**16)**

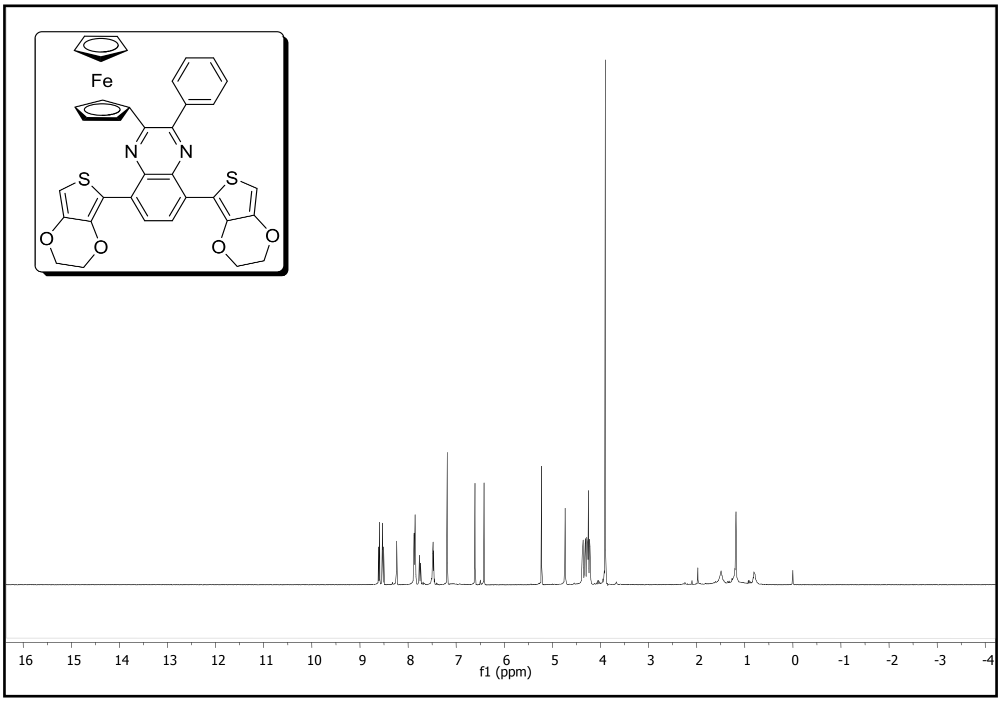

Figure A. 17 ^{1}H-NMR spectrum of 5, 8-bis (2, 3-dihydrothieno [3, 4-b][1,4]dioxin-5-yl)-2-(phenyll)-3-ferrocenylquinoxaline (**M2)**

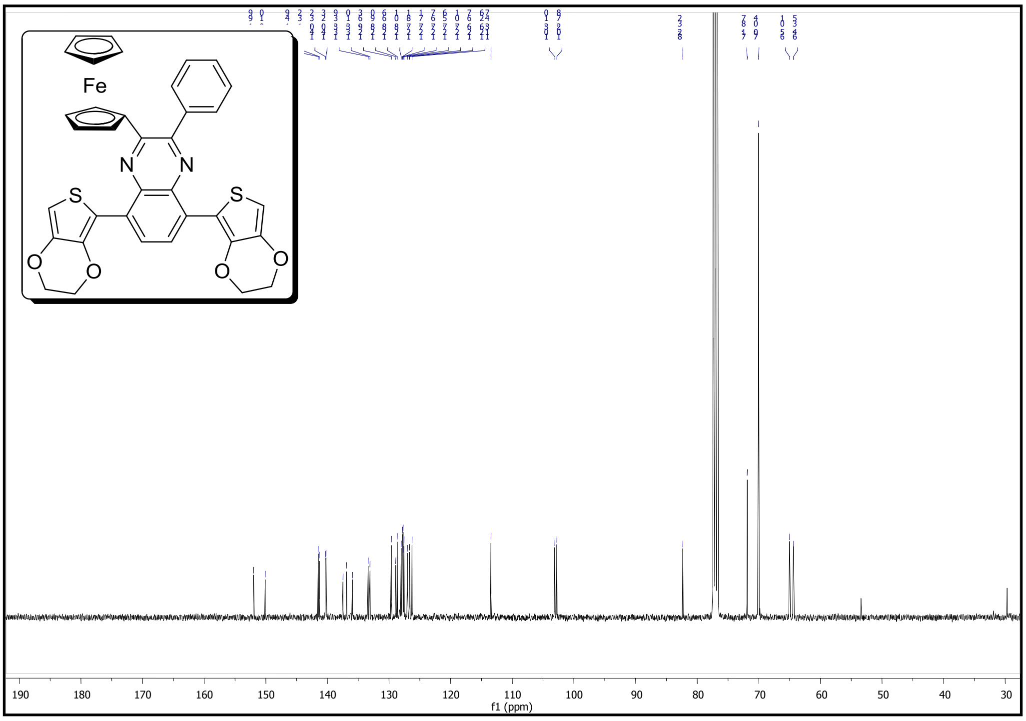

Figure A. 18 ^{13}C-NMR spectrum of 5, 8-bis (2, 3-dihydrothieno [3, 4-b][1,4]dioxin-5-yl)-2-(phenyll)-3-ferrocenylquinoxaline **(M2)**

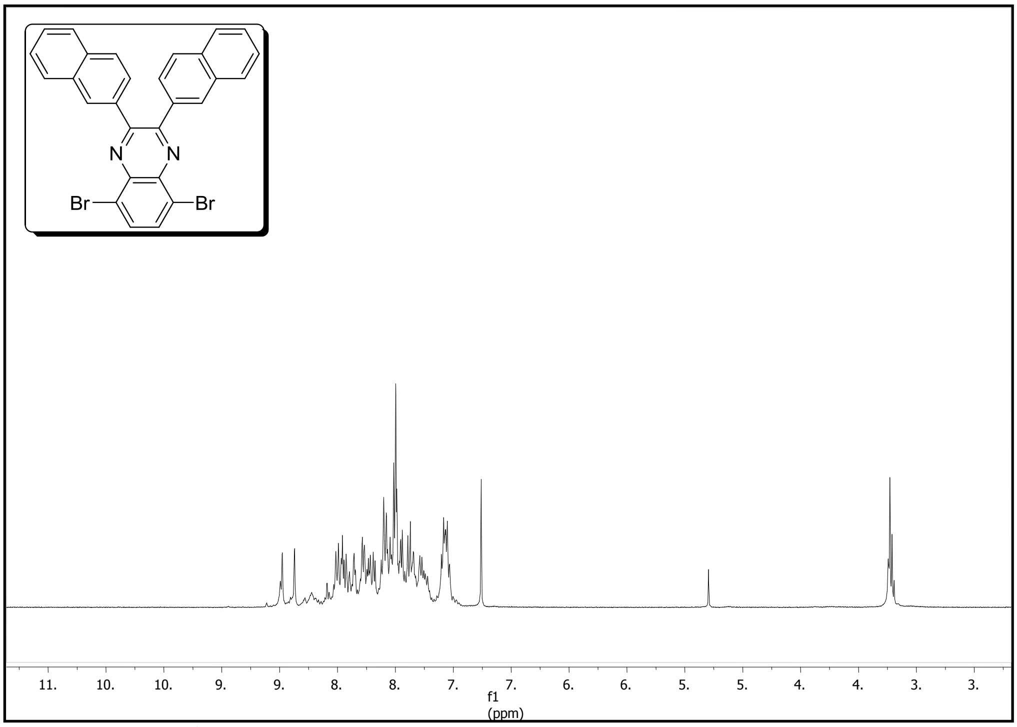

Figure A. 19 ^{1}H-NMR spectrum of 5,8-dibromo-2,3-di(naphthalen-2-yl)quinoxaline (**17)**

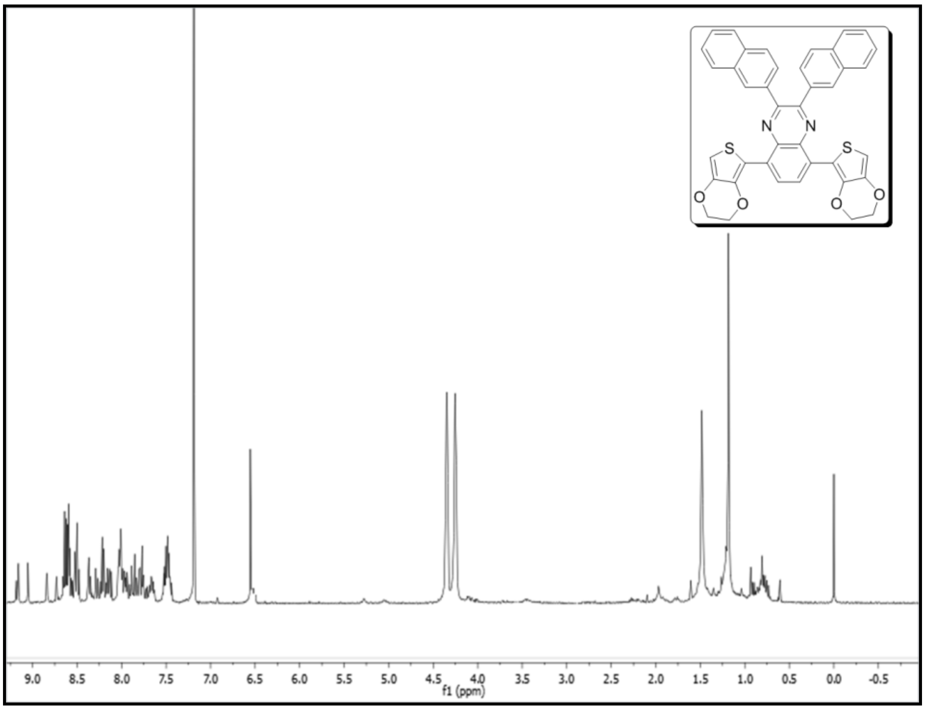

Figure A. 20 ^{1}H-NMR spectrum of 5,8-bis(2,3-dihydrothieno[3,4-b][1,4] dioxin-5-yl)-2,3-di(naphthalen-2-yl)quinoxaline **(M3)**

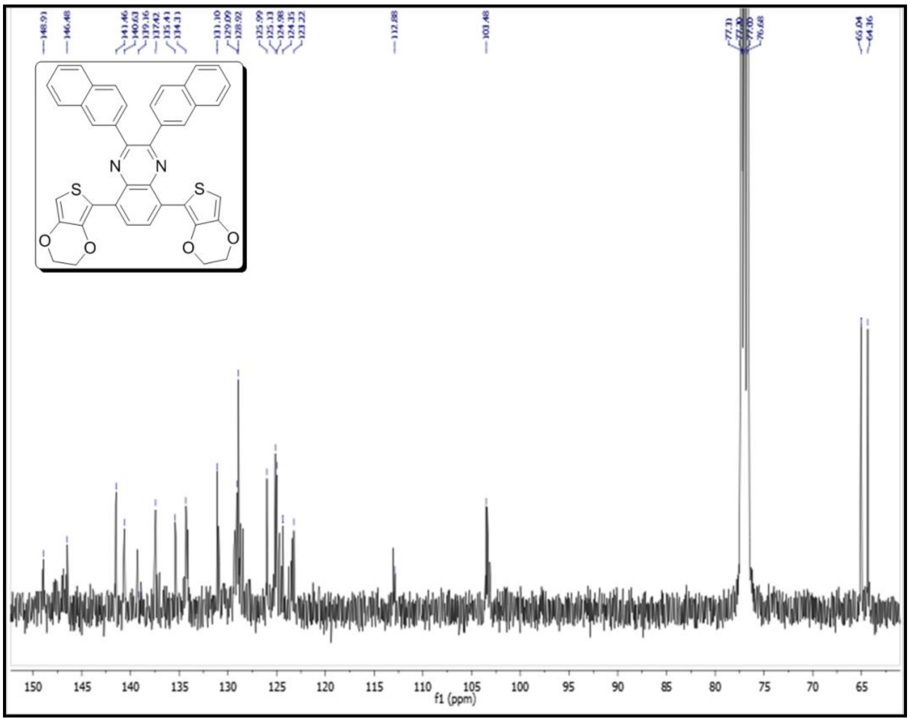

Figure A. 21 ^{13}C-NMR spectrum of 5,8-bis(2,3-dihydrothieno[3,4-b][1,4]dioxin-5-yl)-2,3-di(naphthalen-2-yl)quinoxaline **(M3)**